Energy Conversion and Management 242 (2021) 114294

Contents lists available at ScienceDirect

Energy Conversion and Management

journal homepage: www.elsevier.com/locate/enconman

Techno-economic analysis of supercritical carbon dioxide cycle integrated with coal-fired power plant

Dhinesh Thanganadar [a], Faisal Asfand [a,b], Kumar Patchigolla [a,*], Peter Turner [a]

[a] School of Water, Energy and Environment (SWEE), Cranfield University, Cranfield MK43 0AL, UK
[b] The School of Computing and Engineering, University of Huddersfield, Huddersfield HD1 3DH, UK

ARTICLE INFO

Keywords:
Supercritical CO_2 cycle
Fossil-fired
Techno-economic
Cost of electricity
Multi-variable optimisation

ABSTRACT

Supercritical carbon dioxide (sCO_2) cycles can achieve higher efficiencies than an equivalent steam Rankine cycle at higher turbine inlet temperatures (>550 °C) with a compact footprint (tenfold). sCO_2 cycles are low-pressure ratio cycles (~4–7), therefore recuperation is necessary, which reduces the heat-addition temperature range. Integration of sCO_2 cycles with the boiler requires careful management of low-temperature heat to achieve higher plant efficiency. This study analyses four novel sCO_2 cycle configurations which capture the low-temperature heat in an efficient way and the performance is benchmarked against the state-of-the-art steam Rankine cycle. The process parameters (13–16 variables) of all the cycle configurations are optimised using a genetic algorithm for two different turbine inlet temperatures (620 °C and 760 °C) and their techno-economic performance are compared against the advanced ultra-supercritical steam Rankine cycle. A sCO_2 power cycle can achieve a higher efficiency than a steam Rankine cycle by about 3–4% points, which is correspond to a plant level efficiency of 2–3% points, leading to cost of electricity (COE) reduction. Although the cycle efficiency has increased when increasing turbine inlet temperature from 620 °C to 760 °C, the COE does not notably reduce owing to the increased capital cost. A detailed sensitivity study is performed for variations in compressor and turbine isentropic efficiency, pressure drop, recuperator approach temperature and capacity factor. The Monte-Carlo analysis shows that the COE can be reduced up to 6–8% compared to steam Rankine cycle, however, the uncertainty of the sCO_2 cycle cost functions can diminish this to 0–3% at 95% percentile cumulative probability.

1. Introduction

A flexible thermal power plant has a significant role in the future energy view to maximise higher penetration of variable renewable energy generation into the grid. National Energy Technology Laboratory (NETL), USA is funding researches to develop flexible fossil-fuel power plants with the integration of thermal energy storage [1]. Supercritical carbon dioxide (sCO_2) cycles are investigated to enhance the plant performance and flexibility owing to their compact footprint [2]. Indirect sCO_2 cycles aren't only investigated for coal-fired plant [3], but also for CSP applications [4], nuclear [5], combined cycle power plant [6], waste heat recovery [7], geothermal [8]. Semi-closed, direct-fired sCO_2 cycles such as Allam cycles can be integrated with a coal-fired plant by adapting a commercial gasification unit. Moreover, additional technological challenges need to be addressed such as high-pressure combustor design and the corrosion and erosion issues caused by the impurities in coal and particulates [9]. Various indirect cycle configurations have been proposed for different applications and Crespi et al. [10] had reviewed forty-two cycle configurations. Thanganadar et al. [6] has integrated five cascade cycle configurations with the bottoming cycle, and the study showed that the cascade cycles can be integrated with a sensible heat source with a larger temperature difference across the primary heat exchanger (ΔT). Conventionally, the Brayton cycles are thermodynamically compared using efficiency vs specific power curves with the objective of maximising both of them [11]. The typical cost share of the boiler is about 30–50 % of the whole plant cost whilst the other systems including turbine, feed water heater, steam piping, and cooling system covers the remaining [12]. This indicates that increasing the efficiency not only reduces the fuel cost but also reduces the size of the boiler (reducing the boiler heat duty) for a given electrical power output, thus strongly reducing the capital cost. In addition, turbomachinery are volumetric devices, therefore reducing the volumetric flow can reduce their size and cost, increasing the specific power for a given fluid. Therefore, maximising both of them is expected to minimise the cost of electricity (COE).

* Corresponding author.
E-mail address: k.patchigolla@cranfield.ac.uk (K. Patchigolla).

https://doi.org/10.1016/j.enconman.2021.114294
Received 20 December 2020; Accepted 12 May 2021
Available online 30 May 2021
0196-8904/© 2021 The Author(s). Published by Elsevier Ltd. This is an open access article under the CC BY license (http://creativecommons.org/licenses/by/4.0/).

Nomenclature

CIT	Compressor Inlet Temperature
HT	High Temperature
HTR	High Temperature Recuperator
IC	Intercooler
COE	Cost of Electricity
LT	Low Temperature
LTR	Low Temperature Recuperator
MC	Main Compressor
MH	Main Heater
GA	Genetic Algorithm
PC	Precooler
PCC	Partial Cooling Cycle
PR	Pressure ratio
PreC	Pre-compressor
RC	Recompressor
RCBC	Recompression Brayton Cycle
RH	Reheater
sCO_2	supercritical Carbon Dioxide
TASC	Total as Spent Capital
TIT	Turbine Inlet Temperature
TPC	Total Plant Cost

sCO_2 cycles are generally more efficient than an equivalent steam Rankine cycle when the turbine inlet temperature (TIT) is > 550 °C [5]. The closed-loop sCO_2 cycle is inefficient without recuperation as the cycle pressure ratio is small (around 4–7) owing to the higher critical pressure of CO_2; 73.8 bar. The effectiveness of the recuperation circuit is limited by the occurrence of a pinch point as the thermodynamic properties of sCO_2 varies dramatically, limiting the maximum heat transfer. A recompression cycle (RCBC) is highly efficient as it has two recuperators and the cold stream capacitance of the low temperature recuperator (LTR) is controlled by a parallel recompression loop, which is analogous to direct mixing recuperation. However, the ΔT is lower (220 °C) for this cycle due to the smaller pressure ratio, leading to lower specific power. Therefore, integration of this cycle with a coal-fired power plant might not be able to cool the flue gas close to the required air preheater (APH) temperature, thereby penalising the boiler efficiency. Alternatively the ΔT of a simple recuperative cycle and partial cooling cycle is about 285 °C for a TIT of 750 °C at 300 bar [13] which makes them attractive, though the efficiency of the former cycle is lower. Miller et al. [14] suggested that the maximum temperature limitation of APH is 371 °C based on vendor information, which is unlikely to be achieved with the standard proposed cycles, therefore, alternative cycle configurations are investigated. The partial cooling cycle has a higher ΔT with a small penalty in efficiency, therefore this cycle could offer a lower CAPEX configuration [15]. Cascade cycles can accept the heat over a large temperature range; however, the efficiency of these cycles is generally lower [16]. Therefore, these cycles are less attractive for applications where internal recycling of the hot source is possible, increasing the mean Carnot heat addition temperature, such as nuclear and CSP [16]. Sun et al. [17] proposed to integrate a bottoming cycle in the low-temperature flue gas path of a coal fired power plant and investigated five sCO_2 cycles as a bottoming cycle solution, concluding that recompression and partial cooling cycles better matches the temperature profile. Low temperature thermal management is crucial for sCO_2 cycles particularly when integrated with sensible heat sources. For instance, Mohammadi et al. [18] proposed a triple power cycle concept for a combined cycle power plant to better utilise the low-temperature heat from the flue gas. For a coal-fired plant, the flue gas has to be cooled to the maximum APH temperature limit in order to maximise the plant efficiency, therefore, the cascade cycles and their variants can be attractive depending on the ΔT requirement. Miller at.al. [14] showed that the theoretical maximum efficiency of cascade cycles is 27% and 32% whilst the maximum efficiency of RCBC is 34% and 34.5% when the TIT is 593 °C and 730 °C respectively. Also, despite having three primary heat exchangers as opposed to one in RCBC without low-grade heat recovery, the cost of the cascade cycle was lower than the base cycle whilst the cost of RCBC was roughly twice for a TIT of 593 °C [14]. On the other hand, the cost index of the cascade cycle increases almost in a similar manner for both cascade cycle and RCBC for a TIT of 730 °C, which implies that the cycle selection can be primarily affected by the TIT. Thanganadar et al. [19] showed that sCO_2 recompression cycle off-design efficiency and the heat input to the cycle reduces significantly for a higher ambient temperature operation when maximising the efficiency, which is critical for coal-fired power plants. Thanganadar et al. [20] also showed that the off-design heat input reduction to the cycle for the partial cooling cycle is lesser than recompression cycle when maximising the cycle efficiency at higher ambient temperature operations, making partial cooling cycle attractive.

Qiao Zhao [21] performed a superstructure based optimisation to explore the optimal cycle configuration and concluded that the selection of compressor inlet temperature doesn't influence the optimal layout selection based on cycle efficiency whilst the TIT impacts the efficiency without notable changes in component size, within the investigated search space. The superstructure was formulated by combining the a few sCO_2 cycles and the optimal configuration to maximise efficiency favours two-stage reheating, double recompression and a preheater tapping from the main compressor outlet for low-grade heat recovery [22]. On the other hand, a lower Levelised Cost of Electricity (LCOE) solution is achieved with an intercooled single-reheat simple recuperative cycle with low-grade heat management, despite achieving lower efficiency. Mercheri et al. [23] integrated RCBC and their variants with coal-fired plant concluded that sCO_2 cycles can achieve an efficiency of about 47.8% (LHV) and single reheater offers 1.5% pts increase in efficiency whilst double reheat and double recompression increases the efficiency by 0.3 and 0.5%pts respectively. Yann Le Moullec [3] has integrated a sCO_2 cycle with and without post-combustion carbon capture (monoethanolamine as solvent) and showed that a net efficiency of 41.3% (LHV) is achievable when the CO_2 is compressed to 110 bar. Bai et al. [24] has proposed to have three recuperators and a branching stream from the cold outlet of the second stage recuperator is supplied for the boiler low-grade thermal management, concluding that a net cycle efficiency of 49.5% LHV (assumed boiler efficiency of 97%) can be achievable with 296 bar and 650 °C. Park et al. [25] analysed four sCO_2 cycles for coal-fired power plant concluding that maximum efficiency of 43.9% HHV is achieved, which is increased to 45.4% HHV by the addition of transcritical CO_2 (tCO_2) bottoming cycle. Michalski et al. [26] integrated three advanced power cycles including sCO_2 recompression cycle with calcium looping coal-fired power plant, concluding that sCO_2 cycle achieved 0.9% higher efficiency than equivalent steam Rankine cycle. Wei et al. [27] performed a techno-economic analysis of sCO_2 cycle integrated coal/biomass fired power plant with oxy-combustion, concluding that efficiency of 30.5% is achievable using coal as a fuel at a cost of 84.2 €/MWh.

Huang and Sonwane [28] has modelled a double recuperation recompression Brayton cycle and concluded that the TIT is the main driver to increase the efficiency than the turbine inlet pressure. However, increasing the cycle pressure ratio also helps increase the cycle specific power and thereby helps in reduction of CAPEX. Therefore, the optimal pressure and temperature selection is a trade-off between thermodynamic efficiency and economic cost factors. Alfani et al. [29] performed a multi-objective optimisation of a 100 MWe recompression

sCO_2 cycle integrated with the coal-fired plant to investigate the trade-off between system performance and plant flexibility concluding that the sCO_2 cycles half the response time with a 2%pts higher efficiency than conventional steam cycles. White et al. [30] analysed the thermodynamic trend of sCO_2 integrated with the coal-fired power plant that gives insight to the component size (volumetric flow rate for turbomachinery and heat duty for heat exchangers) and efficiency as a function of cycle pressure ratio. A NETL report by White et al. [31] analysed the techno-economic performance of indirect sCO_2 cycles using an oxy-fired circulating fluidized bed, concluding that increasing TIT from 620 °C to 760 °C increased the plant efficiency by 4.4–4.8% pts. The efficiency boost due to the inclusion of intercooler and reheater is more pronounced at 620 °C than at 760 °C. The COE reduces with the addition of an intercooler for both 620 °C and 760 °C whilst the addition of a reheater reduces the COE at 620 °C but slightly increases the COE at 760 °C mainly due to the increased high-temperature piping cost. White et al. [32] integrated a sCO_2 cycle with a NETL baseline commercial air-fired pulverised boilers (B12A) and oxygen-fired circulating fluidized bed for a TIT of 620 °C and 760 °C. This study concluded that the efficiency increased by 5% pts compared to the NETL baseline pulverised coal power plant with an advanced ultra-supercritical steam Rankine cycle (AUSC), and reduced the water consumption by 22–33% owing to the reduction in sink heat duty and the elimination of boiler blowdown. A downdraft boiler is considered for AUSC to reduce the high energy nickel steam piping length between boiler and turbine, consequently reducing cost [33]. Nathan et al. [34] integrated a sCO_2 cycle with an Oxy-CFB boiler and highlighted that the sCO_2 piping cost is higher than an equivalent steam cycle as the mass flow rate is higher. Therefore, increasing the cycle specific power is desired in order to reduce the power cycle component cost by reducing the recuperator heat duty and turbomachine volumetric flow rate. In most of the studies, boiler low-grade heat is managed by a branching-off stream from the sCO_2 cycle or by the integration of a bottoming cycle. However, other options such as increasing the pressure ratio to increase the heat addition ΔT has seldom been investigated, even though the cycle specific power is increased [30]. In particular, partial cooling cycles are known to offer better off-design performance than a recompression cycle for a higher CIT mainly because the turbine exhaust pressure and main compressor inlet pressures are disconnected by the partial compressor in the former case, whilst they only differ by the pressure drop of the recuperators in the latter case [15,35]. Since the pressure ratio of the partial cooling cycle is higher than a recompression cycle for a given maximum pressure, partial cooling cycle performance can be less sensitive to an absolute boiler pressure drop than RCBC, which is critical for a coal-fired boiler [15]. The partial cooling cycle variants are seldom investigated for coal-fired applications although the heat addition ΔT and specific power are higher compared to RCBC [13]. Secondly, in most of the above studies the boiler isn't modelled and a fixed boiler efficiency is considered in the literature. Boiler efficiency is notably dependent on the flue gas exit temperature. For example, every 22 °C increase in the flue gas outlet temperature from the APH reduces the boiler efficiency by 1% [14,36]. Therefore, a whole plant model, which integrates both the boiler and sCO_2 power cycle, need to be modelled and optimised to comprehend the realistic performance of sCO_2 cycles.

This paper investigates four novel thermodynamic cycle configurations, which are the variants of recompression, partial cooling cycle, and cascade cycle for two different TITs (620 °C and 760 °C). The steam condition of an ultra-supercritical steam Rankine (USC) cycle is about 620 °C [32] (above 620 °C high-strength nickel alloy tubes are desired [37]) whilst AUSC operates around 760 °C [33,38], therefore these two operating temperatures are considered for investigation. Both the boiler and sCO_2 cycle are modelled to capture the thermodynamic interactions. A detailed techno-economic analysis is performed for these cycles and the process parameters are optimised using multivariable metaheuristic procedure based on a genetic algorithm for both the TIT's (2×4 cases). The number of continuous process variables ranges from 13 to 16 which significantly complicates the optimisation. The cycle performances are compared against the equivalent baseline NETL steam Rankine cases to benchmark the performance improvements. In order to quantify the risk of developing sCO_2 cycles, a Monte Carlo analysis is performed to assess the cumulative probability distribution of COE due to the uncertainty associated with the cost function of sCO_2 technology. Finally, a sensitivity study is performed for changes in the turbomachinery efficiency, LTR approach temperature, primary heat exchanger pressure drop, and capacity factor.

2. sCO_2 cycle configurations

Four novel sCO_2 cycle configurations were developed in this study by combining the features of recompression (RCBC), partial cooling (PCC) and cascade cycles. Case1 and 2 were developed by integrating a partial cooling cycle with a cascade cycle and the difference between them is the number of recuperators and economiser, i.e. Case 1 has two recuperator/economiser whereas Case 2 contains three. Case 3 and Case 4 integrates a recompression cycle with a cascade cycle and the number of recuperators/ economisers are two for the former case and three for the latter case.

2.1. Cycles derived from PCC (Case 1 and 2)

Fig. 1 shows Case 1 configuration which combines a partial cooling cycle with a cascade cycle (Cascade Cycle 3 [6]) with a two-stage intercooler and a single-stage reheater. The selection of a single-stage reheater and two-stage intercooler is according to White et al. [32]. The main heater (MH) and the reheater (RH) are located in parallel to the flue gas stream so that the flow fraction can be optimised, thereby enable the functionality of adding/removing the reheater into the process. The turbine outlet of HT2 is in the supercritical vapour phase as opposed to the supercritical state in Case 3 and Case 4.

The expanded sCO_2 from the 2nd stage turbine (HT2) is passed through two-stages of recuperation i.e. HTR and LTR respectively. The hot stream outlet of the LTR is partially cooled in a precooler, then compressed above the critical pressure using a precompressor (PreC). A fraction of the outlet stream is compressed using a recompressor and connects downstream of the LTR whereas the remaining flow is cooled at the intercooler and compressed using two-stage intercooler main compressors.

A fraction of the flow downstream of the main compressor is passed through the LTR, whilst the remaining passes through the economiser#2 (Eco2). The LTR cold stream outlet is mixed with the recompressor outlet, followed by mixing with the Eco2 outlet stream, and part of the flow is split to the economiser #1 (Eco1), whilst the remaining flow goes through the HTR. The outlet of the HTR and Eco1 are mixed and a fraction of the flow is passed through a low temperature (LT) turbine while the remaining flow passes thought the main heater, then partially expanded in the 1st HT turbine (HT1), followed by the RH and a 2nd stage expansion in HT2. Fig. 2 shows the typical T-Q diagram of Case 1, where the temperature matching between the cold and hot streams can be compared, inferring the exergy destruction.

Fig. 3 shows the configuration of Case 2 that has three recuperators and economisers as opposed to two in Case 1. This cycle is developed for two reasons, 1) to provide an additional degree of freedom which facilitates the better matching of the T-Q profile (Fig. 4) in the recuperator and primary heat exchanger, reducing the exergy destruction 2) to reduce the heat load of the HTR, which uses an expensive material when the maximum temperature goes over 550 °C, so that the cost of recuperators can be lowered. It should be noted that the former tends to reduce the log-mean temperature driving force, resulting in an increase of conductance, thus the surface area for a given heat duty, therefore a trade-off is required. Fig. 4 shows the typical T-Q diagram of Case 2.

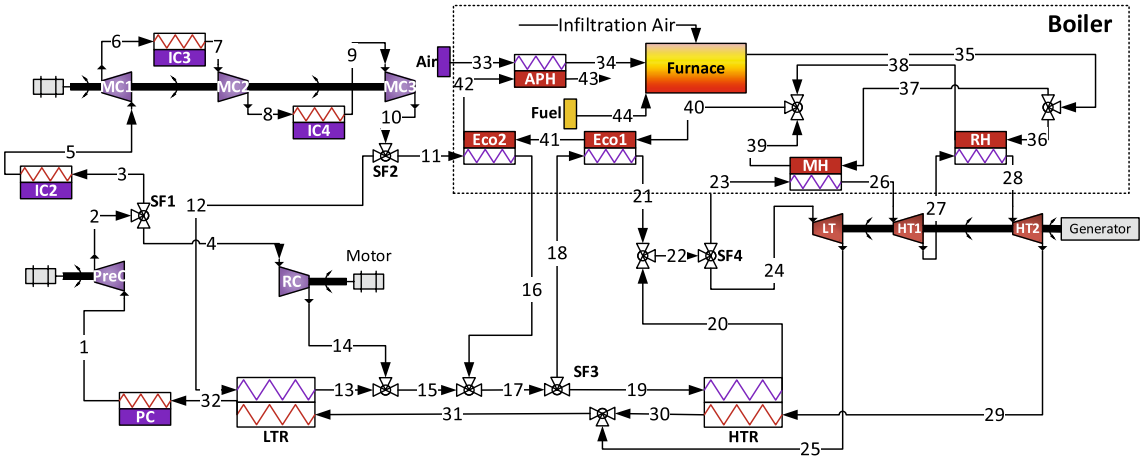

Fig. 1. Process Configuration of Case 1.

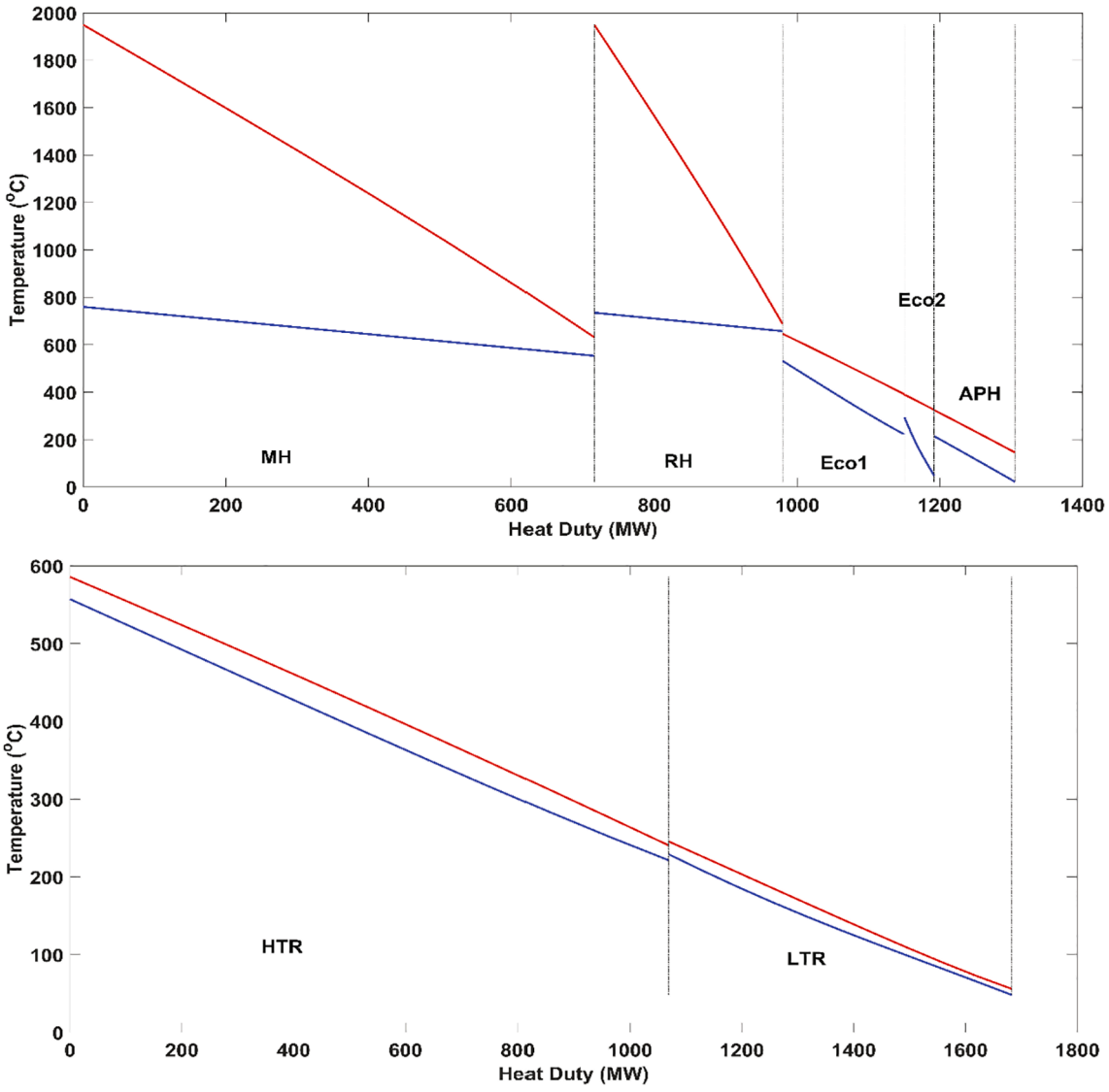

Fig. 2. Temperature-Enthalpy (T-Q) diagram of Case 1, Top) primary heat exchanger train bottom) recuperator train.

2.2. Cycles derived from RCBC (Case 3 and 4)

The recuperator and boiler side components of cycle 3 are similar to Case 1; the only difference is on the heat rejection and compression side components. The cycle configuration 3 combines the features of RCBC and cascade cycles with the two-stage intercooler compressor and

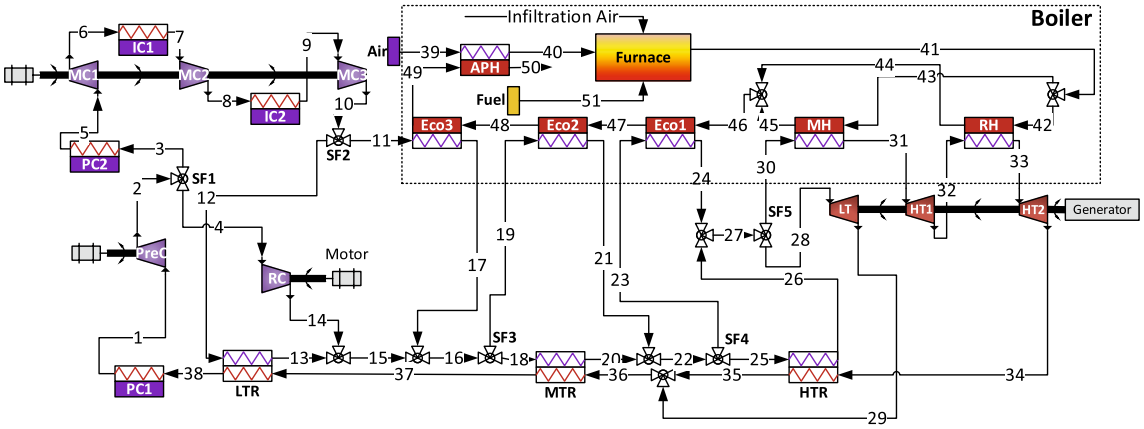

Fig. 3. Process Configuration of Case 2.

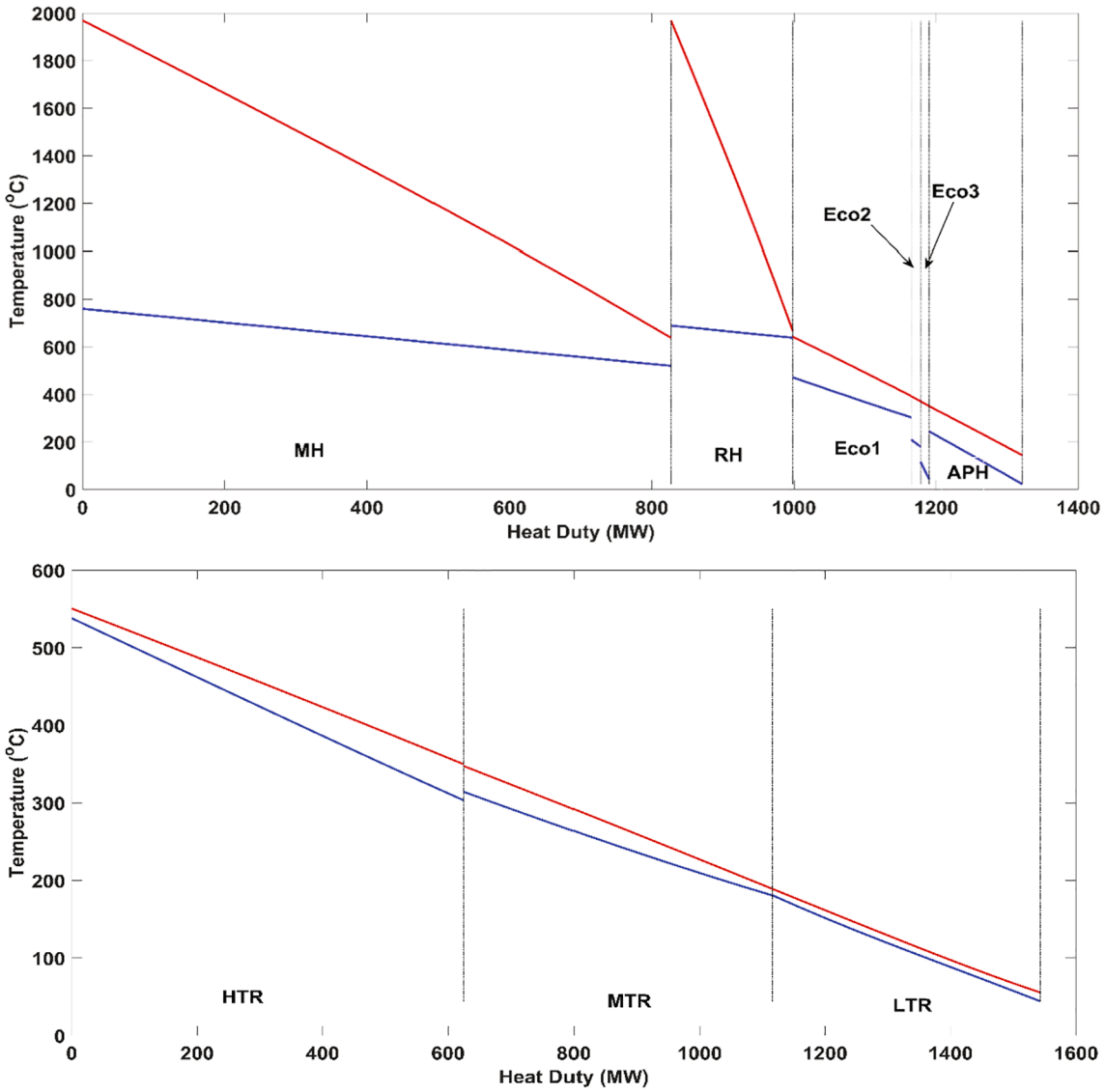

Fig. 4. Temperature-Enthalpy (T-Q) diagram of Case 2, Top) primary heat exchanger train bottom) recuperator train.

single-stage reheater (Fig. 5). Removing the low temperature turbine (LT) changes this configuration close to the alternative configuration studied in White et al. [32]. The expanded sCO_2 from the 2nd stage turbine (HT2) is passed through two-stages of recuperation i.e., HTR and LTR respectively, then part of the sCO_2 flow is diverted through a recompressor (RC) which connects to the LTR cold outlet, bypassing the

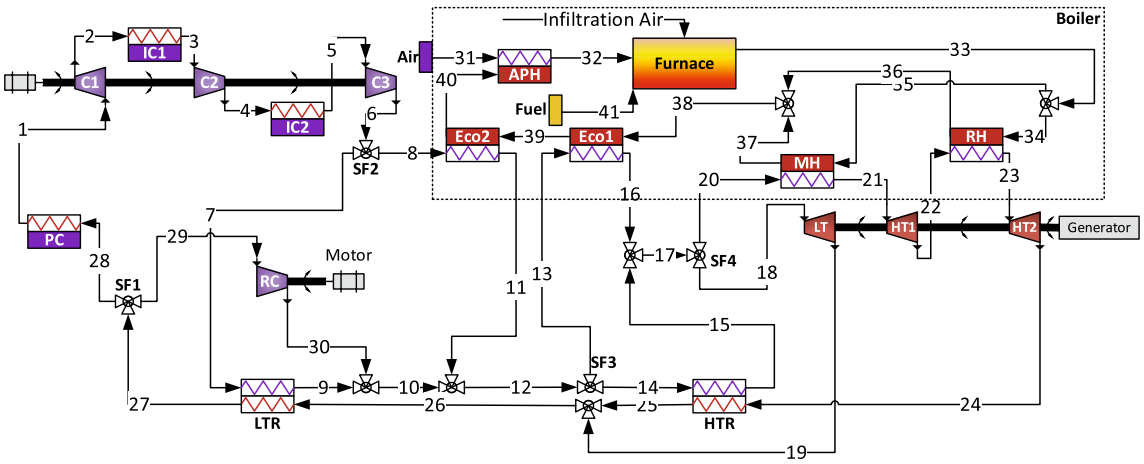

Fig. 5. Process Configuration of Case 3.

LTR cold stream. The remaining flow is passed through the precooler (PC), then it is compressed in a two-stage intercooler compressor and part of the flow is passed through the LTR, whilst the remaining passes through economiser#2 (Eco2).

The LTR cold stream outlet is mixed with the recompressor outlet followed by mixing with the Eco2 outlet stream, and part of the flow is split to the economiser #1 (Eco1), whilst the remaining flow goes through the HTR. The remaining process on the high temperature side is similar to Case 1. The temperature-heat duty (T-Q) diagram of the low temperature recuperator (LTR), high temperature recuperator (HTR)

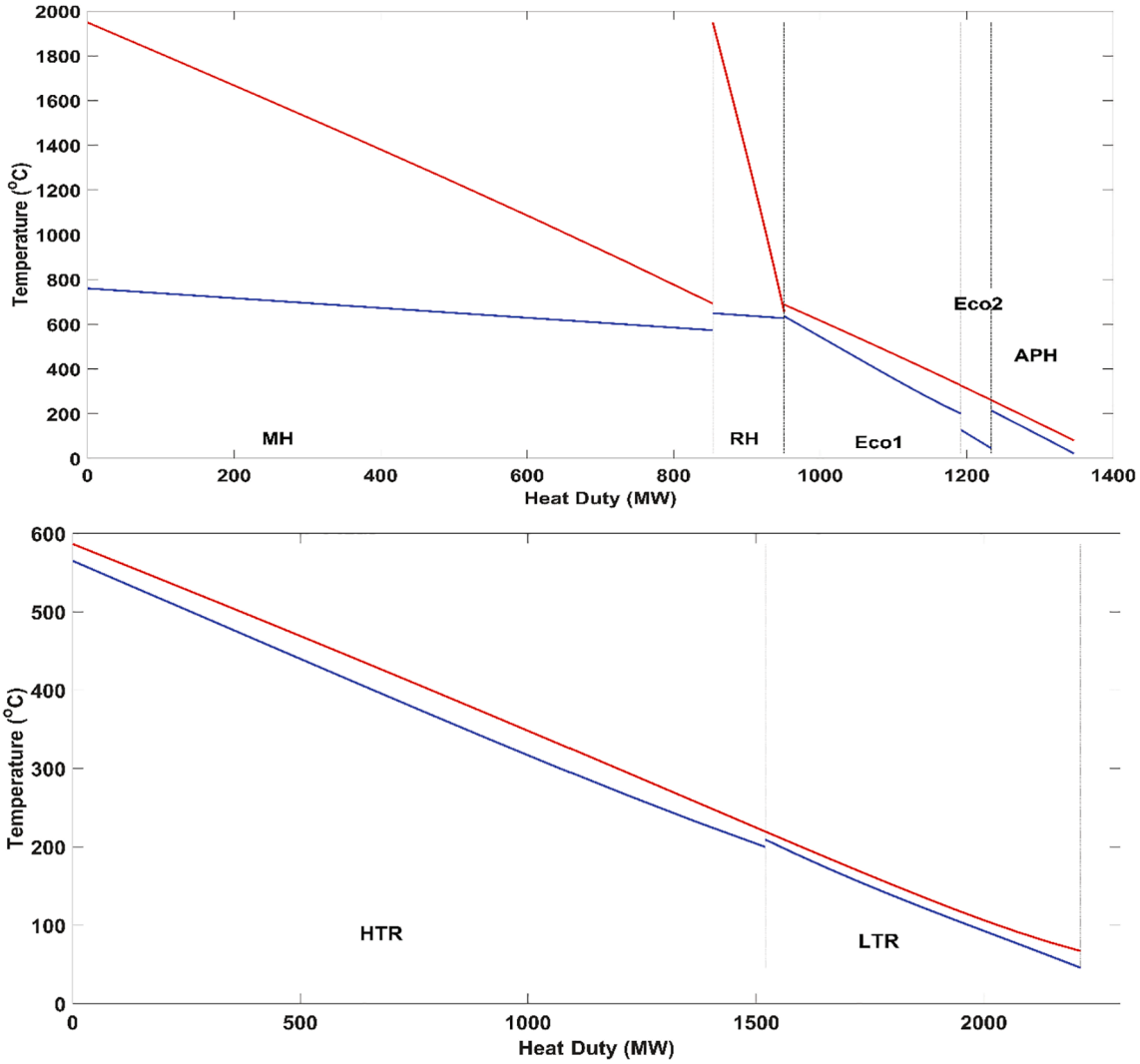

Fig. 6. Temperature-Enthalpy (T-Q) diagram of Case 3, Top) primary heat exchanger train bottom) recuperator train.

and boiler heaters are shown in Fig. 6. Fig. 7 shows the cycle configuration 4 (Case 4) is derived from cycle 3 by adding an additional medium temperature recuperator (MTR) and economiser #3 (Eco3). For the sake of completeness, the T-Q diagram of cycle 4 is shown in Fig. 8.

3. Thermodynamic modelling

An in-house code has been developed in MATLAB® for all the process components such as compressor/ pump, turbine, heat exchanger (one-dimensional), valve, splitter and mixer. The plant-level code sequentially solves the component models in a flexible way, which allows modelling any plant configuration in a robust manner. For a simulation of the closed-loop cycles or recycle streams, the plant solver guesses the tear stream values and converges the solution within the predefined tolerance using a non-linear iterative solver, which is the Newton-Raphson iterative method and Broyden algorithm for calculation of the Jacobian matrix. The thermal physical properties of sCO_2 are calculated using the REFPROP library [39], which uses an iterative routine minimising Helmholtz free energy. The number and the location of the tear streams changes depending on the process configurations.

Since this work adapts the NETL base case steam boiler (B12A) to a sCO_2 based cycle, the fuel input and the air mass flow are fixed as the same as B12A. The ultimate analysis of the Illinois No.6 coal is shown in Table 1. The coal flow is 49.8 kg/s and the primary airflow, secondary airflow and the infiltration airflow are 121.7 kg/s, 396.1 kg/s and 8.7 kg/s respectively [40].

Steady-state mass and energy conservations are applied to all the components to calculate their outlet state properties from the inlet conditions. The recuperators are modelled based on effectiveness while the cooler and the primary heater are modelled based on the outlet temperature set points.

The sCO_2 turbomachinery is simulated as a zero-dimensional model based on their isentropic efficiencies (η_{isen}) The outlet enthalpy (h_{out}) of the turbine is calculated using Eq. (1) and the compressor is calculated using Eq. (2), where h_{2s} is a function of outlet pressure (P_{out})and inlet entropy (s_{in}).

$$h_{out,turb} = h_{in,turb} - (h_{in,turb} - h_{2s,turb}) \times \eta_{isen,turb} \tag{1}$$

$$h_{out,comp} = h_{in,comp} + \frac{h_{2s,comp} - h_{in,comp}}{\eta_{isen,comp}} \tag{2}$$

The heat exchanger is a one-dimensional code in order to capture the nonlinear property variation of sCO_2 along the length of the heat exchanger (10 zones). The number of zones is selected based on an initial set of simulations that captures the nonlinear property variation across the length of the heat exchanger with the computational speed. The heat exchanger function sizes the heat exchanger based on effectiveness (ϵ) using Eq. (3) or specifying the outlet temperature of either the hot or cold stream.

$$\epsilon = \frac{\dot{Q}}{\dot{Q}_{max}} \tag{3}$$

The actual amount of heat transfer (Q) is calculated from the given input of effectiveness and calculated $\dot{Q}_{max}$. The $\dot{Q}_{max}$ is calculated based on Eq. (4).

$$\dot{Q}_{max} = \min(C_{cold}, C_{hot}) \times (T_{h,in} - T_{c,in}) \tag{4}$$

The capacitance rate of the cold stream ($C_{cold} in \frac{W}{K}$) is calculated based on Eq. (5) and a similar equation can also be applied to calculate the hot stream capacitance rate (C_{hot}).

$$C_{cold} = m_{cold} \times \frac{h_{c,in} - h_{c,out,max}}{T_{c,in} - T_{c,out,max}} \tag{5}$$

where the $h_{c,out,max} = f(P_{c,out}, T_{c,out,max})$ and $T_{c,out,max} = T_{h,in}$

The conductance (UA) is calculated for all the heat exchanger zones using the NTU method [41] and the total conductance is the sum of the conductance of all the zones. The heat duty of the heat exchanger is reduced if the minimum pinch temperature constraint is violated within the heat exchanger or any temperature crossover is detected. The primary heat exchanger and the cooler are modelled based on the cold and hot outlet temperatures respectively. For example, $T_{h,in}$ in Eq. (4) is replaced with the desired hot outlet setpoint for the cooler and the heat duty is reduced if the minimum pinch requirement is violated. The economiser outlet temperatures are optimised to maximise the plant efficiency. For the primary heat exchanger, air and flue gas properties are calculated using REFPROP.

3.1. Modelling assumptions

Thermodynamic modelling assumptions are listed in Table 2. All the cycle configurations are simulated for two sets of turbine inlet temperatures (TITs), i.e., 620 and 760 °C.

Table 3 shows the auxiliary power breakdown considered and the cooling water pump, cooling tower fan power is scaled as a function of both precooler and intercoolers duty. Since the thermal input to the boiler is maintained as the same as the B12A base case, the auxiliary power related to fuel/ash handling and flue gas treatment systems is not affected whereas the transformer losses are scaled as a function of the generator gross power output.

3.2. Economic modelling

The COE is calculated by using Eqs. (6) and (7), where *CCF* is the

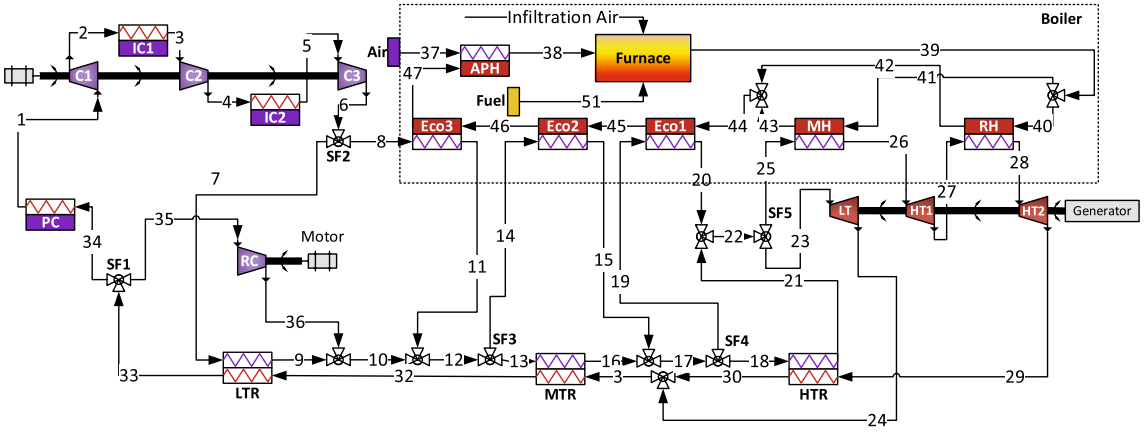

Fig. 7. Process Configuration of Case 4.

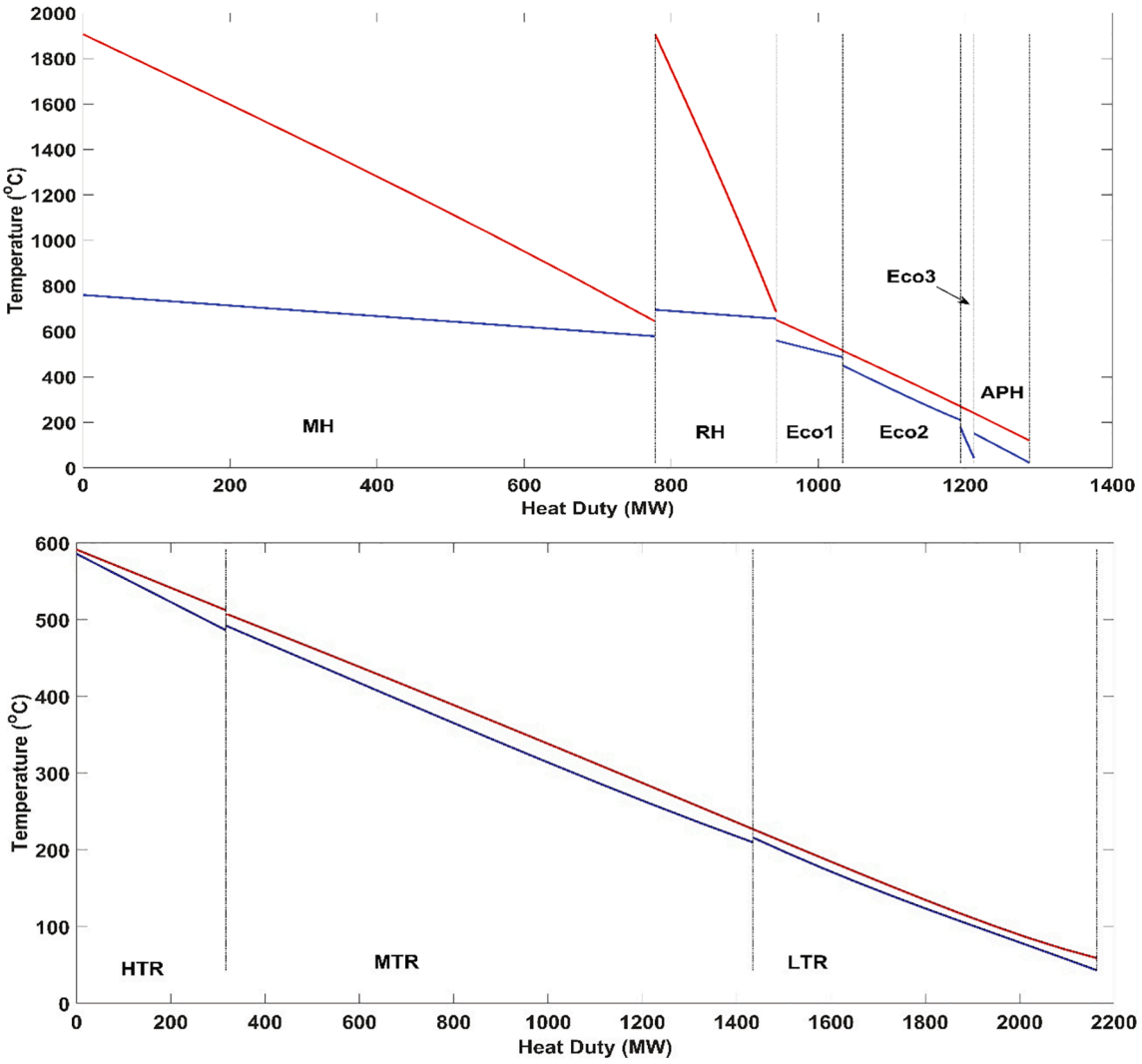

Fig. 8. Temperature-Enthalpy (T-Q) diagram of Case 4, Top) primary heat exchanger train bottom) recuperator train.

Table 1
Coal Specification (Illinois No.6 coal) [40].

Parameter	Unit	Value
High Heating Value (HHV)	kJ/kg	27,113
Low Heating Value (LHV)	kJ/kg	26,151
Ultimate Analysis		
Moisture	Weight%	11.12
Carbon	Weight%	63.75
Hydrogen	Weight%	4.5
Nitrogen	Weight%	1.25
Chlorine	Weight%	0.29
Sulfur	Weight%	2.51
Ash	Weight%	9.7
Oxygen	Weight%	6.88

capital charge factor using a value of 0.102 [40], and a capacity factor (CF) of 85%.

$$COE = \frac{capitalcharge + fixedoperatingcost + variableoperatingcost}{annualnetenergygenerated} \quad (6)$$

$$COE = \frac{CCF^{*}TASC + OC_{fixed} + CF \times OC_{variable}}{CF \times MWh} \quad (7)$$

The total as spent capital (TASC) is calculated using Eq. (8), where the TASC multiplier is taken as 1.134 [43].

$$TASC = TASCMultiplier \times TOC \quad (8)$$

The total overnight cost (TOC) is calculated using Eq. (9). Since the TOC is calculated at the base year, TASC expressed in mixed- year current dollars, spread over the capital expenditure period.

$$TOC = OwnersCost + TPC \quad (9)$$

The owner's cost is calculated using the same breakdown provided in the NETL steam cycle baseline report [40] so that the cycles can be compared.

The total plant cost (TPC) is calculated by using Eq. (10),

$$TPC = BEC + Contingencies + H.O.Fee \quad (10)$$

The home office (H.O.) fee is assumed as 10% of the bare erected cost (BEC) [40], and 15% of the BEC is considered as the project contingency [40]. The process contingency is neglected to be in line with the cost estimation of the NETL base case B12A.

The BEC includes the equipment, material and both the direct and indirect labour costs. Since fuel supply to the boiler is fixed as same as base case (B12A) value, the cost of fuel handling, ash handling and other subsystem cost are constant. On the other hand, the size and the cost of the cooling water system, boiler and the turbine building cost change for different configurations. The scaling method is applied to the NETL base cost structure to account the cost variation for the changes in the

Table 2
Thermodynamic modelling assumptions.

Description	Unit	Value
Turbine isentropic efficiency [32]	%	92.7
Main compressor isentropic efficiency [32]	%	85
Recompressor isentropic efficiency [32]	%	85
Pre-compressor isentropic efficiency [32]	%	85
Recuperator Effectiveness [6]	%	95
Recuperator minimum pinch [32]	°C	5.6
High Pressure (Main Compressor Outlet) [32]	bar	350
Precooler/intercooler outlet temperature	°C	32
Turbine Inlet Temperature [33]	°C	620,760 (Varied)
Boiler minimum pinch temperature	°C	30
Economiser minimum pinch temperature	°C	30
Ljungström APH minimum pinch temperature	°C	30
Maximum flue gas temperature to APH [14]	°C	371
Minimum flue gas outlet temperature from APH [40]	°C	142.8
Pre-cooler approach temperature [42]	°C	15
Intercooler approach temperature [42]	°C	15
Cold side pressure drop of Precooler	%	1
Hot side pressure drop of Precooler	%	0.8
Cold side pressure drop of intercooler	%	1
Hot side pressure drop of intercooler	%	0.1
Cold side pressure drop of Primary Heat Exchanger	%	1
Hot side pressure drop of Primary Heat Exchanger	%	1
Cold side pressure drop of economiser	%	0.3
Hot side pressure drop of economiser	%	0.3
Cold side pressure drop of Recuperator	%	0.3
Hot side pressure drop of Recuperator	%	0.8
Generator efficiency [40]	%	98.5

Table 3
Auxiliary Power Breakdown [40].

System	Unit	Value	Scaling
Coal Handling and Conveying	kW_e	430	Thermal Input (B12A)
Pulverizers	kW_e	2690	
Sorbent Handling & Reagent Preparation	kW_e	850	
Ash Handling	kW_e	620	
Primary Air Fans	kW_e	1330	
Forced Draft Fans	kW_e	1700	
Induced Draft Fans	kW_e	6660	
Selective Catalytic Reduction (SCR)	kW_e	40	
Activated Carbon Injection	kW_e	22	
Dry sorbent Injection	kW_e	86	
Baghouse	kW_e	90	
Wet Flue Gas Desulphurisation (FGD)	kW_e	2830	
Miscellaneous Balance of Plant	kW_e	2000	Constant
Steam Turbine Auxiliaries	kW_e	400	
Condensate Pumps	kW_e	800	
Ground Water Pumps	kW_e	460	
Circulating Water Pumps	kW_e	4520	Condenser Duty
Cooling Tower Fans	kW_e	2340	
Transformer Losses	kW_e	1820	Gross Power

reference parameter as shown in Eq. (11). Table 4 shows the scaling parameter, reference parameter, cost reference and the exponent used [44,45].

$$cost_{scaled} = cost_{reference}\left(\frac{scalingparameter}{referenceparameter}\right)^{exponent} \quad (11)$$

The cost functions of the sCO_2 power block components are listed in Table 5, where the temperature correction factor (f), material and labour cost are also shown [46–48]. The estimation of the high-temperature sCO_2 piping and foundation are scaled from the sCO_2 cycle NETL report [31]. Since the piping material and turbine foundation cost changes with temperature, the reference cost, reference parameter values change for the two TITs considered. The fuel price of 2.94 $/MMBTU is considered [40] and the fixed and variable operation and maintenance (O&M) costs breakdowns are estimated using the procedure given in the NETL baseline report [40].

4. Metaheuristic optimisation

A single-objective optimisation was performed to explore the maximum thermal performance for changes in the boundary conditions. Genetic algorithm (GA) is used which maximises the plant net efficiency ($\eta_{boiler} \times \eta_{cycle}$) by optimising the power cycle process variables including pressure(s), mass flow rate, economiser outlet temperatures, and split fractions. Table 6 shows the optimisation parameters and their ranges used for each of the four sCO_2 cycles, obtained from a set of initial runs. The minimum/maximum bounds were adjusted if a variable reached close to their bounds at the optimal solution. The process flow models are integrated with GA in MATLAB® to perform the optimisation study and the structure of the code is shown in Fig. 9. The number of population and the number of generations are selected between 15 and 20 times the numbers of variables to ensure global convergence. Two constraints are considered in the optimisation 1) the maximum flue gas inlet temperature to APH is 371 °C (commercial availability [14]), 2) the minimum flue gas outlet temperature of APH is 142.8 °C (same as B12A base case [40]). The components are modelled in a flexible way to handle a wide range of inputs. For instance, the optimisation algorithm can set a compressor outlet pressure lower than its inlet pressure in which case the compressor acts as a pressure reducing valve and the outlet temperature is calculated using the isenthalpic process. Similarly, if the cold outlet temperature of an economiser set by GA is lower than its cold inlet temperature or the hot inlet temperature is lower than the cold inlet temperature plus the minimum pinch, then the economiser will be bypassed and the pressure drop is set to zero. In this way, the thermodynamic process code is flexible to handle a wide range of search space without it failing.

5. Model validation

The modular in-house code was validated against the literature in the author's previous works [19,20] and additional validation is shown in this section. Moisseytsev and Sienicki [49] reference cycle condition is used for validation which shows the design data of 96 MW_e sodium-cooled fast reactors. The sCO_2 cycle configuration is a recompression cycle with a TIT of 471.8 °C is modelled in MATLAB. Although the turbine and compressor isentropic efficiencies weren't reported, they have been back calculated from the outlet temperature values stated. These resulted in efficiencies of 93.3%, 90.7% and 93.5% for the main compressor, recompressor and turbine respectively. Generator efficiency of 98.5% and a mechanical loss of 1% are considered for both the turbine and compressors. The state temperature differences are matching with the literature reported values with the maximum relative percentage error of 0.2% as shown in Table 7.

6. Results and discussion

6.1. Thermal performance comparison

All the four cases are optimised for two different turbine inlet temperatures (TITs), i.e., 620 °C and 760 °C. In order to distinguish both the simulation results, a suffix "a" is added for 620 °C results and "b" is added for 760 °C results. For instance, Case1a refers to the simulation results of Case1 for a TIT of 620 °C whereas Case1b refers a TIT of 760 °C.

The thermodynamic performance of all the four cases for a TIT of 620 °C and 760 °C is shown in Table 8. Since the amount of fuel supplied is kept the same as the steam Rankine base case (B12A), maximising the plant net efficiency also maximises the net power output. The maximum sCO_2 power cycle efficiency ($\eta_{cycle} = \frac{NetPower}{Heatinput_{cycle}}$) achieved for a TIT of 620 °C is 49.3% (Case 2a), which is increased to 53% (Case 1b) when the TIT increased to 760 °C. The heat input to the cycle ($Heatinput_{cycle}$) is the sum of the heat duty of the main heater, reheater and all the

Table 4
Bare Erected Cost (BEC) functions and scaling method for sCO_2 cycle [40,44].

Item No.	Description	Reference Cost for 620 °C (k $) [40]	Scaling Parameter [44]	Scaling exponent [44]	Reference Value	Unit
1	Coal & Sorbent Handling	45,397	Fixed	NA	NA	NA
2	Coal & Sorbent Prep & Feed	21,531	Fixed	NA	NA	NA
3	Feedwater & Miscellaneous BOP Systems					
3.1	Feedwater System	36,316	NA	NA	NA	NA
3.2	Water Makeup & Pre-treating	9079	Fixed	NA	NA	NA
3.3	Other Feedwater Subsystems	12,184	NA	NA	NA	NA
3.4	Service Water Systems	2104	Fixed	NA	NA	NA
3.5	Other Boiler Plant Systems	20,387	NA	NA	NA	NA
3.6	FO Supply Sys & Nat Gas	897	Fixed	NA	NA	NA
3.7	Waste Treatment Equipment	7145	Fixed	NA	NA	NA
3.8	Misc. Equip. (Cranes, Air Comp., Comm	5532	Fixed	NA	NA	NA
4	Boiler & Accessories	Calculated from Power cycle Table 5				
5A	Gas Clean-up & Piping	167,272	Fixed	NA	NA	NA
7	Duct work & Stack	45,629	Fixed	NA	NA	NA
8	sCO_2 Power Cycle					
8.1, 8.2, 8.3	Power block components: compressors, recuperator, coolers, turbines, Auxiliaries	Calculated from power cycle Table 5				
8.4	sCO_2 Piping [31]	90,132	Mass flow rate	0.7	3674	kg/s
8.5	TG Foundations [31]	6156	Gross power	0.71	685,265	kW
9	Cooling Water System					
9.1	Cooling tower	16,814	Cooling duty	0.74	609,002	kW
9.2	Circulating water pump	2732	Cooling duty	0.73	609,002	kW
9.3	Circ. Water System Auxiliaries	803	Cooling duty	0.63	609,002	kW
9.4	Circ. Water Piping	11,906	Cooling duty	0.63	609,002	kW
9.5	Make-up Water System	1526	Fixed	–	–	NA
9.6	Component Cooling Water Sys.	1068	Cooling duty	0.63	609,002	kW
9.7	Circ. Water Foundations & Structures	9187	Cooling duty	0.58	609,002	kW
10	Ash & Spent Sorbent Handling Systems	16,778	Fixed	–		NA
11	Accessory Electric Plant					
11.1	Generator Equipment	2664	Gross power	0.57	685,265	kW
11.2	Station Service Equipment	5184	Auxiliary Power	0.43	29,688	kW
11.3	Switchgear & Motor	5352	Auxiliary Power	0.43	29,688	kW
11.4	Control Conduit & Cable Tray	13,831	Auxiliary Power	0.43	29,688	kW
11.5	Wire & Cable	17,352	Auxiliary Power	0.43	29,688	kW
11.6	Protective Equipment	1658	Fixed	NA	NA	NA
11.7	Standby Equipment	1854	Gross power	0.46	685,265	kW
11.8	Main Power Transformers	12,163	Gross power	0.46	685,265	kW
11.9	Electrical Foundations	1678	Gross power	0.69	685,265	kW
12	Instrumentation & Control	26,316	Auxiliary Power	0.13	29,688	kW
13	Improvements to Site	16,394	Bare Erected Cost	0.2	1,030,996	k$
14	Buildings & Structures					
14.1	Boiler Building	23,566	Bare Erected Cost	0.09	1,030,996	k$
14.2	Turbine Building	34,597	Bare Erected Cost	0.12	1,030,996	k$
14.3	Administration Building	1827	Bare Erected Cost	0.1	1,030,996	k$
14.4	Circulation Water Pump house	457	Gross power	0.6	609,002	kW
14.5	Water Treatment Buildings	1576	Fixed	NA	NA	NA
14.6	Warehouse	993	Bare Erected Cost	0.1	1,030,996	
14.7	Machine Shop	806	Bare Erected Cost	0.1	1,030,996	
14.8	Other Buildings & Structures	609	Bare Erected Cost	0.1	1,030,996	
14.9	Waste Treating Building & Str.	2540	Fixed	NA	NA	NA

Table 5
sCO_2 cycle cost functions [47,48].

Component	Cost Function ($)	Temperature Correction Factor (−)	Installation Cost Percentage (%)	
			Material	Labour
Compressor	$1,230,000 * P^{0.3992}$	*NA*	8	12
Turbine	$182,600 \times P^{0.5561} \times f$	$f = \begin{cases} 1, T < 550 \\ 1 + 1.106e^{-4}(T-550)^2, T \geq 550 \end{cases}$	8	12
Recuperator	$49.45 \times UA^{0.7544} \times f$	$f = \begin{cases} 1, T < 550 \\ 1 + 0.02141(T-550), T \geq 550 \end{cases}$	2	3
Precooler	$32.88 \times UA^{0.75}$	*NA*	8	12
Primary Heat Exchanger	$820,800 \times Q^{0.7327} \times f$	$f = \begin{cases} 1, T < 550 \\ 1 + 5.3e^{-6}(T-550)^2, T \geq 550 \end{cases}$	50	

economisers. This is equivalent to an increase of about 3.5–3.6%pts higher than the equivalent steam Rankine cycle. The maximum plant net efficiency on HHV basis ($\eta_{boiler} \times \eta_{cycle} = \frac{NetPower}{Fuelmassflow \times HighHeatingValue}$) is 43.5% and 46.9% (Cases 1a and 1b), which corresponds to an increase of 3.4%pts over the steam Rankine cycle. This implies increasing the TIT can aid in reducing the COE if the benefits due to the increased efficiency are not compensated by the increased capital cost owing to the use of high-temperature alloy materials. Inclusion of a third recuperator (Case

Table 6
Variable ranges of parameters considered in optimisation.

Parameter	Unit	PCC		RCBC	
		Minimum bound	Maximum bound	Minimum bound	Maximum bound
Pre-compressor Inlet Pressure	bar	50	60	NA	NA
1st stage maincompressor Inlet Pressure	bar	75	100	75	90
2nd stage maincompressor Inlet Pressure	bar	120	175	120	175
3rd stage maincompressor Inlet Pressure	bar	175	250	175	250
HT turbine#1 outlet pressure	bar	120	175	120	175
Economiser#1 cold outlet temperature	°C	300	550	300	650
Economiser#2 cold outlet temperature	°C	100	350	100	450
Economiser#3 cold outlet temperature	°C	100	300	100	350
APH cold outlet temperature	°C	25	370	25	370
Flow split to recompressor	–	0	0.5	0	0.5
Flow split to economiser#1	–	0	0.4	0	0.4
Flow split to economiser#2	–	0	0.6	0	0.6
Flow split to economiser#3	–	0	0.2	0	0.2
Flow split to LT turbine	–	0	0.3	0	0.3
Flue gas flow split to reheater	–	0	0.5	0	0.5
sCO_2 mass flow rate at the inlet of main compressor	kg/s	1600	3000	1600	3000

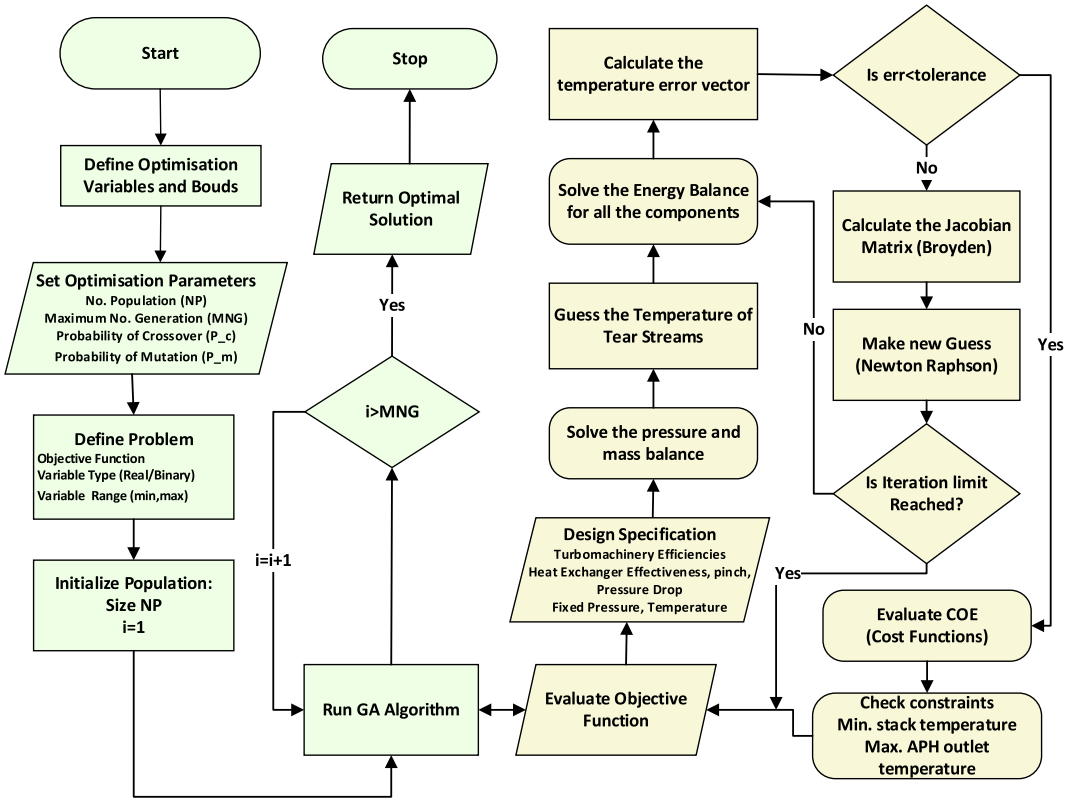

Fig. 9. GA Algorithm flowchart used in this study.

Table 7
Benchmark of the supercritical recompression CO_2 (C3) cycle stream data with Moisseytsev and Sienicki [49].

State	Temperature (°C)			State	Temperature (°C)		
	Literature [49]	This Study	Relative Error (%)		Literature [49]	This Study	Relative Error (%)
1	32.79	32.79	−0.0	7	362.30	362.27	0.0
2	84.40	84.40	−0.0	8	190.70	190.88	−0.1
3	171.80	171.84	−0.0	9	90.20	90.41	−0.2
4	175.20	175.33	−0.1	10	90.20	90.41	−0.2
5	323.30	323.30	0.0	11	90.20	90.41	−0.2
6	471.80	471.80	0.0	12	183.80	184.04	−0.1

Table 8
Thermodynamic performance summary table.

Parameters	Unit	Steam	Partial Cooling Cycle (PCC)		Recompression Cycle (RCBC)	
		B12A	Case 1a	Case 2a	Case 3a	Case 4a
TIT = 620 °C						
Net Power	MW	550.0	586.9	587.3	586.6	587.5
Power cycle efficiency	%	45.7	49.1	49.3	48.8	48.9
Plant Efficiency	%	40.7	43.5	43.5	43.4	43.5
TIT = 760 °C						
		AUSC	Case 1b	Case 2b	Case 3b	Case 4b
Net Power	MW	550.3	633.0	629.8	627.8	632.2
Power cycle efficiency	%	49.5	53.0	52.6	52.4	52.8
Plant efficiency	%	44.1	46.9	46.6	46.5	46.8

2 and Case 4) does not notably increase the efficiency, therefore this may not be economically justified over Case 1 and Case 3 respectively.

Cycles derived from the partial cooling cycle (Case 1 and 2) offered a similar level of efficiency as the cycles derived from a recompression cycle for both the TITs studied. It should be noted that the maximum plant efficiency reported by White et al. [43] is 49.5% HHV, which is higher than value obtained in this study. The reason is that the flue gas exit temperature is constrained to 142.8 °C in this work in order to be in line with the steam base case (B12A). However, White et al. [43] considered a minimum flue gas temperature of 50 °C by implementing in-bed sulphur capture using circulating fluidised bed combustion, which helped to increase the boiler efficiency from ~ 89% to 92.9%. This clearly shows that changing the boiler from pulverised coal-fired with flue gas desulphurisation unit to circulating fluidised bed in-bed with sulphur capture aids in enhancing the plant efficiency by about 2.5% pts. Optimisation of the recompression cycle-based cases closed the split fraction to the LT turbine when maximising the efficiency, which reduces this cycle similar to the White et al. [43] proposed cycle. This is also valid for the cycles derived from partial cooling cycles when maximising the efficiency.

Fig. 10 shows the breakdown of the turbine shaft power of all the four cases for a TIT of 620 °C and Fig. 11 shows the breakdown for a TIT of 760 °C. The turbine shaft power generated for the partial cooling based cycles are higher than recompression cycle as the pressure ratio is higher. For the partial cooling based cycles at 620 °C, the compressive power is about ~ 27–28% of the total turbine shaft power whilst the miscellaneous category accounts for the generator loss and plant auxiliary power (4%). The turbine shaft power for the recompression based cycles are less as the compressive power accounts for about 24–25% for a TIT of 620 °C. The compressive power share is reduced to about 23–24% for partial cooling based cycles when the TIT increased to 760 °C (Fig. 11), whilst it is about 22% for recompression based cycles.

The energy balance of all the eight cases are shown in Table 9 and the Sankey diagram [50] of Case 1a and Case 1b are shown in Fig. 12. The major low-grade heat rejection in the cycle is at the condenser (42–42.6%), followed by the boiler sensible heat loss (about 11–11.7%). The share of auxiliary power and generator loss from the thermal input is 2.1% and 0.7% respectively. The boiler loss has increased by 0.7% (Case 2a) from a minimum value of 11% (Case 3a), which is caused by the higher flue gas exit temperature than the minimum flue gas outlet temperature from APH (i.e., 142.8 °C). When increasing the TIT from 620 °C to 760 °C, the heat rejection at the cooler is reduced (38.7–39.7%) owing to the increased Carnot efficiency at a higher TIT (Table 9). Reducing the cooler heat duty also reduces the amount of water/air required to cool the system; for instance, the mass flow rate of the cooling medium for Case 1b is about 15% lower than B12A. In the case of water-cooled plants, the elimination of boiler blowdown further assists in reducing water consumption.

The recuperator conductance (UA) of all the cycle configurations studied are shown in Fig. 13. Increasing the number of recuperators from two to three (Case 2 and Case 4) also increased the conductance due to the reduced temperature driving force. The conductance of the cycles derived from partial cooling cycles (Case 1 and Case 2) is lower than the recompression based cycles as the heat duty of the former cases is lower than the latter cases by about 25%. This is because the turbine exhaust temperature of partial cooling based cycles are lower than recompression based cycles owing to a higher pressure ratio. Also, the recompression cycle better matches the hot and cold stream temperature profile than a partial cooling cycle, resulting in a reduced temperature driving force. Increasing the TIT from 620 °C to 760 °C reduces the recuperator conductance for partial cooling based cycles whereas they increased for recompression based cycles. Although the plant efficiency of all the four cycles are roughly similar for a TIT of 620 °C, partial cooling cycle is preferred owing to its superior off-design performance than recompression cycle at higher ambient temperatures [20].

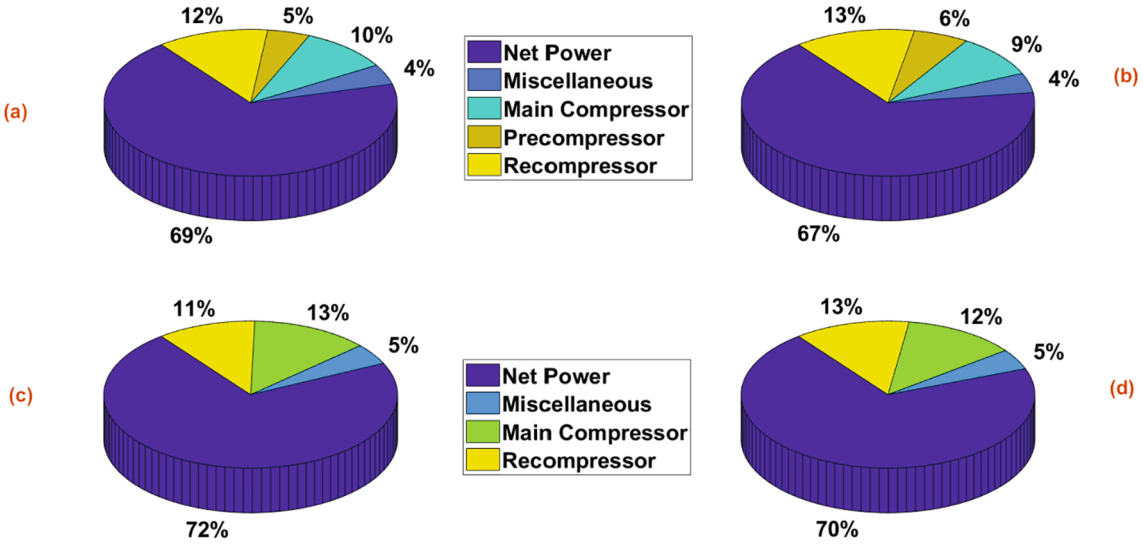

Fig. 10. Turbine power breakdown for a TIT of 620 °C, a) Case 1a, b) Case 2a, c) Case 3a, d) Case 4a.

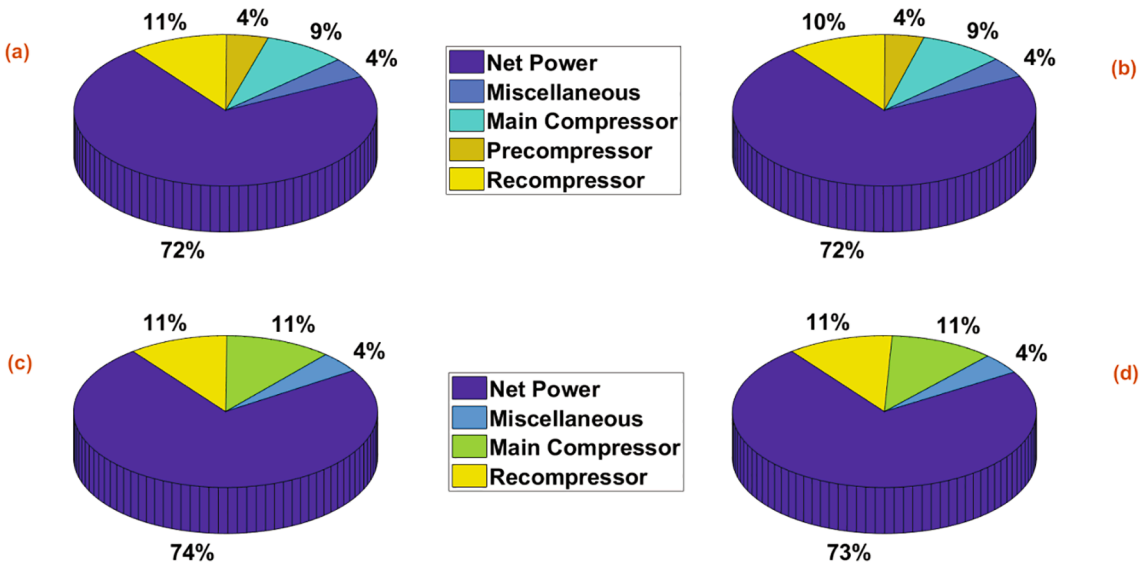

Fig. 11. Turbine power breakdown for a TIT of 760 °C, a) Case 1b, b) Case 2b, c) Case 3b, d) Case 4b.

Table 9
First-law energy balance for both TIT of 620 °C and TIT of 760 °C.

Parameters	Unit	Partial Cooling Cycle (PCC)		Recompression Cycle (RCBC)	
		Case 1a	Case 2a	Case 3a	Case 4a
Fuel input	MW	1350.7 (100%)			
Boiler Loss	%	11.5	11.7	11.0	11.1
Condenser Loss	%	42.2	42.0	42.7	42.6
Auxiliary Power	%	2.1	2.1	2.1	2.1
Generator Loss	%	0.7	0.7	0.7	0.7
Net Power (Net Efficiency)	%	43.5	43.5	43.4	43.5
		Case 1b	Case 2b	Case 3b	Case 4b
Fuel input	MW	1350.7 (100%)			
Boiler Loss	%	11.6	11.4	11.4	11.3
Condenser Loss	%	38.7	39.2	39.4	39.1
Auxiliary Power	%	2.1	2.1	2.1	2.1
Generator Loss	%	0.7	0.7	0.7	0.7
Net Power (Net Efficiency)	%	46.9	46.6	46.5	46.8

6.2. Economic performance

Figs. 14 and 15 shows the total plant cost (TPC) breakdown of the boiler (Item 4 in Table 4) and turbine block (Item 8 in Table 4) for a TIT of 620 °C and 760 °C respectively. This will be referred as power cycle equipment capital cost in this paper as it only includes the cost of boiler, turbine, compressor, recuperator and coolers. Table 10 includes the piping cost and foundation cost. It is worth highlighting that the boiler and turbine shares about 52–60% of the power cycle equipment's capital cost, depending on the cycle configuration, whilst the remaining cost associated with other sub-system are shown in Table 10. The cost share of the boiler and economiser is significantly higher than all the other power cycle equipment's capital cost. For instance, the cost of the boiler (main heater + reheater + economisers) is about 60–67% of the power cycle equipment's capital cost for both the TITs studied. Despite having higher efficiency, the power cycle equipment capital cost is notably increased by about 20% when increasing the TIT from 620 °C to 760 °C for partial cooling based cycles whereas it increased by about 10–16% for recompression based cycles. This clearly shows that the increased efficiency isn't enough to offset the increased power cycle equipment capital cost. However, the capital cost of balance of the plant (BOP) and fuel cost also reduces at higher efficiencies and that may contribute to reducing the COE. The cost share of the compressor is higher than the turbine when the TIT is 620 °C, but the turbine cost share is increased, notably at TIT of 760 °C, owing to the temperature correction factor to account for the change in the materials. The recuperator shares a significant portion of the BEC (16–22%), therefore the selection of the

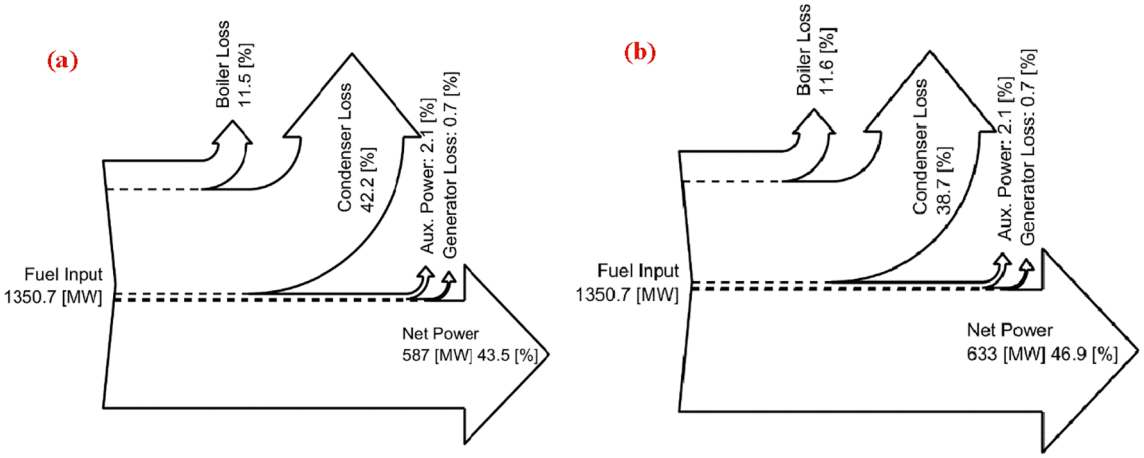

Fig. 12. Energy balance Sankey diagram, a) Case 1a (TIT of 620 °C), b) Case 1b (TIT of 760 °C).

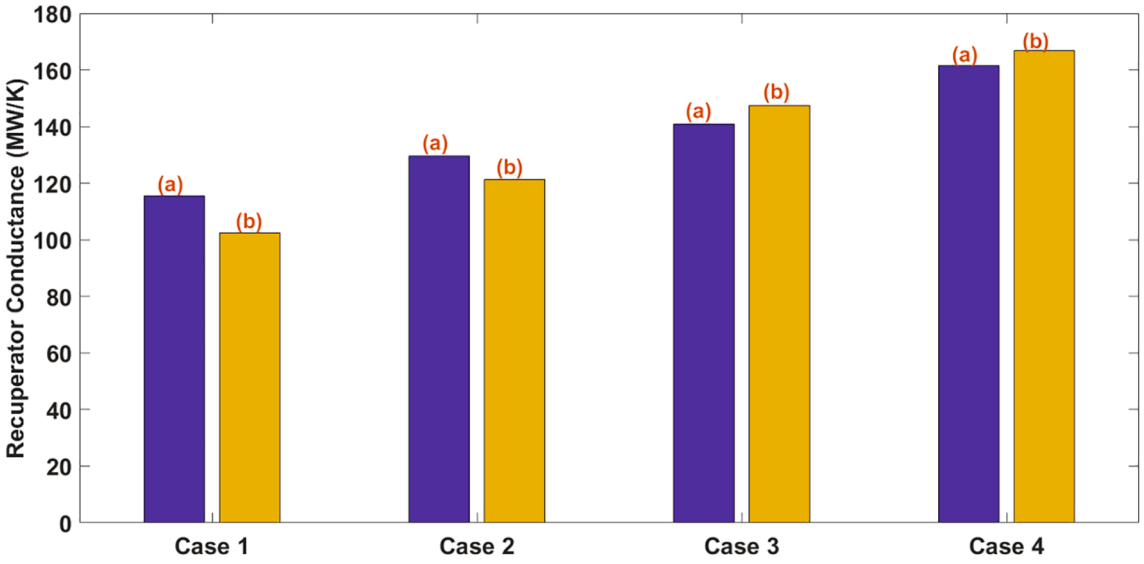

Fig. 13. Recuperator conductance (UA) of all the cycle configurations studied.

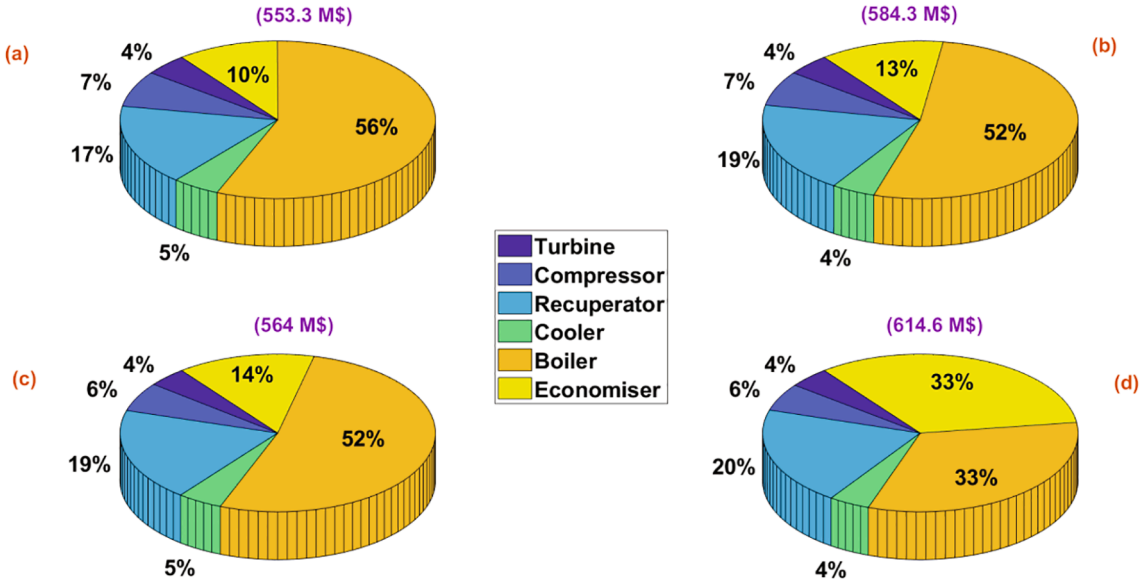

Fig. 14. Capital cost breakdown of boiler and turbine block for a TIT of 620 °C, a) Case 1a, b) Case 2a, c) Case 3a, d) Case 4a.

appropriate approach temperature and pressure drop can significantly influence the overall cost.

Table 10 shows the complete breakdown (similar item parameter as the reference NETL report [40,44]) of the unit TPC for both the TIT (a) and TIT (b) studied. The contribution of power block equipment cost and boiler in the TPC is in the range of 52–60%. The TPC of sCO_2 is higher than equivalent steam Rankine cycle within a range of 1–7% for all the cases for a TIT of 620 °C and 760 °C except for Case 3b where TPC is same as the steam Rankine cycle. The increase capital cost of item 4 and 8 are mainly compensated by the reduced cost of item 3 i.e. feed water and miscellaneous BOP for a TIT of 600 °C. The base case coal input to the AUSC [43] is different from the B12A case as White et al. [43] adjusted the fuel feed in the former case to match the net power output to approximately 550 MW, whilst this study kept the fuel input constant. Therefore, comparing the absolute TPC of AUSC with sCO_2 cycles are not possible, but the normalised TPC with net power output can be compared. The contribution of all the items, except power cycle equipment cost of sCO_2 cycle cases, are lower than equivalent steam Rankine cycle. For a TIT of 760 °C, the increased cost of power cycle equipment is larger than the reduction in cost from other items, resulting in a net increase of TPC. On the other hand, the TPC of Case 1a is lower than B12A by 5.6%.

Fig. 16 shows the breakdown of COE for all the eight cases investigated. It can be seen that a maximum cost reduction of 7.6% can be achieved by using Case 2b compared to B12A, which corresponds to a reduction of 3.4% compared to AUSC. Although the TASC of sCO_2 cycles is almost like steam Rankine cycles, the capital cost contribution on COE is lower due to higher energy generation owing to its increased efficiency. Likewise, the fixed O&M, variable O&M and fuel cost is less than the equivalent steam Rankine cycle owing to the increased amount of energy generation. It should be noted that despite achieving higher efficiency (Table 9), increasing the TIT from (a) to (b) does not noticeably reduce the COE (Fig. 16). However, increasing the cycle efficiency also offers other benefits such as reduction in the cooling water requirement in the cooler and the carbon emission, which are outside the scope of this study.

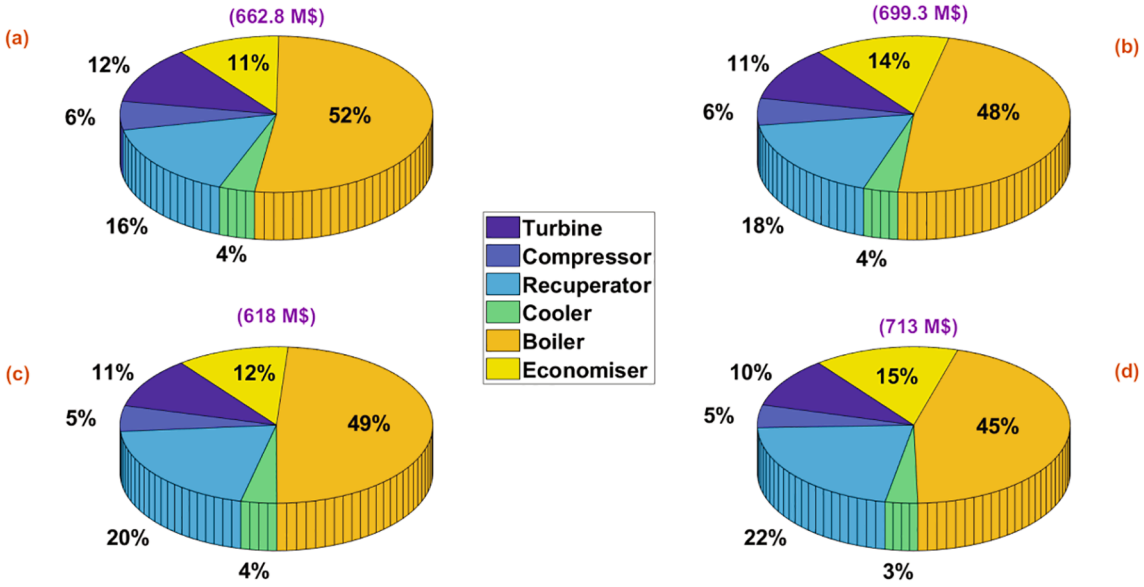

Fig. 15. Capital cost breakdown of boiler and turbine block for a TIT of 760 °C, a) Case 1b, b) Case 2b, c) Case 3b, d) Case 4b.

Table 10
Unit total plant cost (TPC) Summary in $/kW.

Item No	Parameter (TIT = 620 °C)	Unit	B12A [40]	Case 1a	Case 2a	Case 3a	Case 4a
1	Coal & Sorbent Handling	$/kW	82.5	77.3	77.3	77.4	77.3
2	Coal & Sorbent Prep & Feed	$/kW	39.1	36.7	36.7	36.7	36.7
3	Feedwater & Miscellaneous BOP Systems	$/kW	170.3	42.2	42.2	42.2	42.1
4	Boiler & Accessories	$/kW	621.3	628.9	648.5	638.0	688.0
5A	Gas Cleanup & Piping	$/kW	304.1	285.0	284.8	285.2	284.7
7	Duct work & Stack	$/kW	83.0	77.7	77.7	77.8	77.7
8	Steam/sCO_2 Power Cycle	$/kW	303.5	372.1	405.0	388.4	422.5
9	Cooling Water System	$/kW	80.1	71.9	72.3	73.0	72.2
10	Ash & Spent Sorbent Handling Systems	$/kW	30.5	28.6	28.6	28.6	28.6
11	Accessory Electric Plant	$/kW	112.2	107.0	107.5	106.4	106.5
12	Instrumentation & Control	$/kW	47.8	44.6	44.6	44.6	44.5
13	Improvements to Site	$/kW	29.8	28.0	28.1	28.1	28.3
14	Buildings & Structures	$/kW	121.8	113.6	113.8	113.8	114.1
Total Plant Cost (TPC)		$/kW	2,026.1	1913.5	1967.0	1940.1	2023.2
Item No	Parameter (TIT = 760 °C)	Unit	AUSC [43]	Case 1b	Case 2b	Case 3b	Case 4b
1	Coal & Sorbent Handling	$/kW	78.5	71.7	72.1	72.3	71.8
2	Coal & Sorbent Prep & Feed	$/kW	37.1	34.0	34.2	34.3	34.1
3	Feedwater & Miscellaneous BOP Systems	$/kW	145.9	39.1	39.3	39.4	39.2
4	Boiler & Accessories	$/kW	610.7	656.0	688.8	594.3	676.8
5A	Gas Cleanup & Piping	$/kW	286.6	264.2	265.6	266.5	264.6
7	Duct work & Stack	$/kW	81.8	72.1	72.4	72.7	72.2
8	Steam/sCO_2 Power Cycle	$/kW	326.2	506.8	537.1	525.5	582.6
9	Cooling Water System	$/kW	72.3	63.0	63.9	64.6	63.5
10	Ash & Spent Sorbent Handling Systems	$/kW	29.2	26.5	26.6	26.7	26.5
11	Accessory Electric Plant	$/kW	109.3	99.2	99.6	99.6	99.0
12	Instrumentation & Control	$/kW	47.3	41.2	41.4	41.6	41.3
13	Improvements to Site	$/kW	28.4	26.6	26.9	26.7	26.9
14	Buildings & Structures	$/kW	118.6	106.7	107.5	107.3	107.4
Total Plant Cost (TPC)		$/kW	1,972.0	2,007.2	2,075.5	1,971.4	2,105.9

6.3. Monte-Carlo uncertainty analysis

Since the manufacturing experience of sCO_2 power block components is so limited, the uncertainty of them is larger. Therefore, an uncertainty estimation is essential in order to foresee the range of COE with the cumulative probability to reduce the financial risk. The cost functions uncertainty is listed in Table 11, and Monte-Carlo uncertainty analysis is performed for all the eight sCO_2 cases. The total number of samples considered in each cycle COE estimation is 10,000. The uncertainty ranges of all the sCO_2 power cycle cost functions reported by Weiland et al. [47] are used in this study.

Fig. 17 shows the cumulative probability distribution of COE for all eight cases. It clearly shows that the Case 3b and Case 1b are the lowest COE alternatives and the lowest COE of 72 $/MWh is achievable whilst it can be as high as 79.9 $/MWh for Case 3b. This implies that the COE can be reduced by up to 12% at zero cumulative probability and the reduction is only about 3% at the maximum cumulative probability compared to B12A. On the other hand, when comparing against AUSC, Case 3b COE reduces by up to 8% at the minimum cumulative probability while it increases by about 2% at the maximum cumulative probability. This implies that the cost reduction potential of a sCO_2 cycle compared with steam Rankine cycles are within the uncertainty range of the cost functions. Therefore, sCO_2 cycles may reduce the COE of equivalent steam Rankine cycles up to 0–8% depending on the

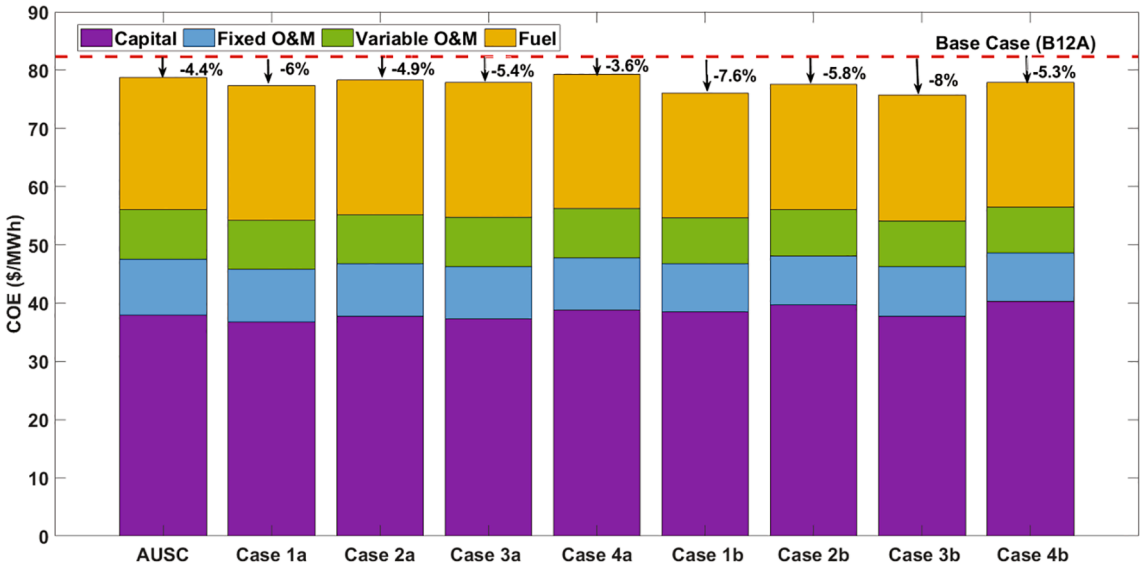

Fig. 16. Cost of Electricity (COE) comparison with steam Rankine cycle (B12A).

Table 11
Component cost uncertainty ranges used in Monte-Carlo simulation.

Component	Minimum	Maximum
Compressor/Pump	0.6	1.48
Turbine	0.75	1.3
PHEX	0.75	1.25
Recuperator	0.69	1.38
Cooler	0.75	1.28

uncertainty of the cost functions. The configurations with three recuperators and economisers are not economical compared to two recuperator cycles. This study excluded the carbon taxing, in which case sCO_2 cycles can offer higher economic benefits as the efficiency of the sCO_2 cycle is higher than the equivalent steam Rankine cycle.

6.4. Sensitivity analysis

sCO_2 cycle performance is sensitive to the component design assumptions including compressor isentropic efficiency, turbine isentropic efficiency, pressure drop and recuperator approach temperature [15]. Therefore, a sensitivity study has been performed for the partial cooling based cycle (Case 1b) and the results are plotted in Fig. 18. The cycle efficiency drops by about 1%pts when increasing the low temperature recuperator approach temperature from 3 to 20 °C. There is a clear cost minimal solution existing below the conductance of the recuperator that exponentially increases but the increase in efficiency cannot offset the increased recuperator cost. The optimal LTR approach temperature is around 10 °C. The change in efficiency for changes in LTR approach temperature has two different slopes pivoting at the minimum cost optimal point. It is well noted that the minimum pinch temperature and effectiveness of the MTR and HTR were kept unchanged at 5.6 °C and 95% respectively.

Since the pressure ratio of sCO_2 cycles is small (~4–7), the cycle performance is very sensitive to pressure drop. For instance, the efficiency drops by about 0.5%pts when the boiler main heater cold side pressure drop increased by 2% (equivalent to ~ 7 bar), which also increased the COE by 0.9$/MWh. The boiler pressure drop of an sCO_2 cycle has to be higher in order to ensure the cooling of the radiant zone

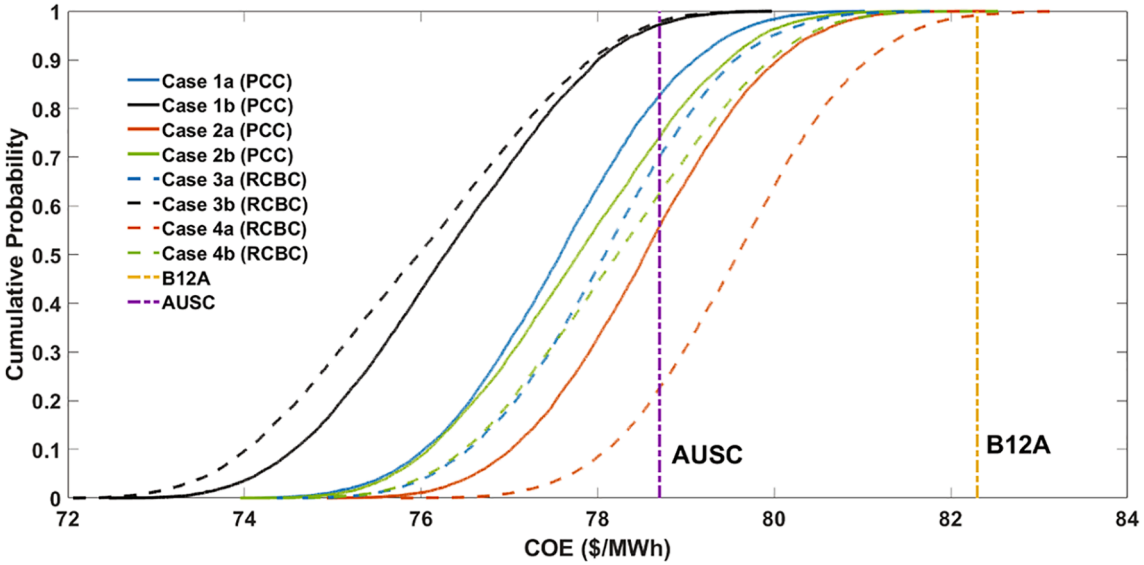

Fig. 17. Cumulative probability distribution of COE from Monte-Carlo analysis.

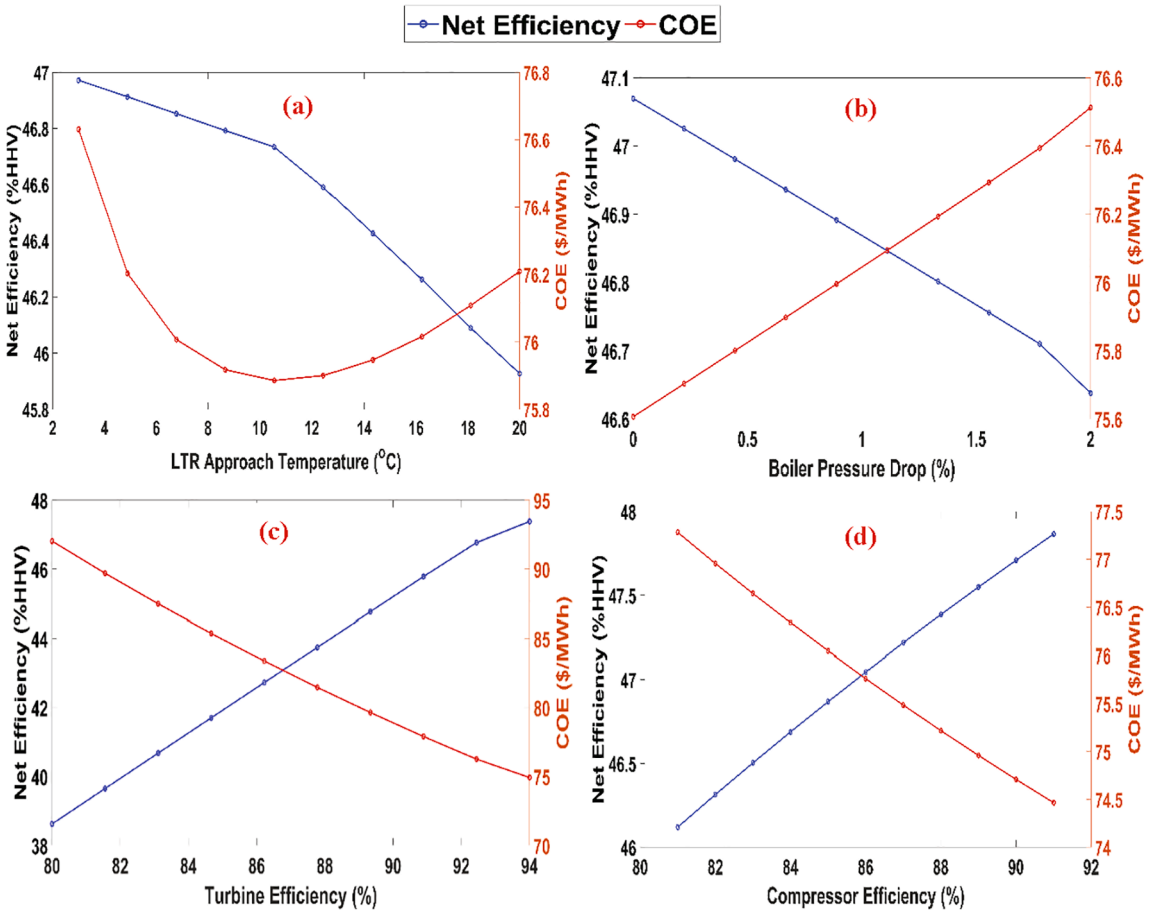

Fig. 18. Sensitivity study of Case 1b a) LTR approach temperature, b) main heater pressure drop c) Turbine isentropic efficiency d) compressor isentropic efficiency.

[15]. The efficiency reduction slope per percentage increase of main heater cold stream pressure drop is 0.2%pts, which corresponds to a reduction of COE by around 0.45 $/MWh. However, this absolute value can change depending on the cycle pressure ratio and main heater inlet pressure.

For the 550 MW plant, the turbine has to be a multi-stage axial type [51] whilst the main compressor can be axial or radial [52,53]. The radial compressor can offer a higher operating range, which is essential for sCO_2 cycles as the variation of the fluid density is significant close to the critical point. Noall and Pasch [54] indicated that a compressor

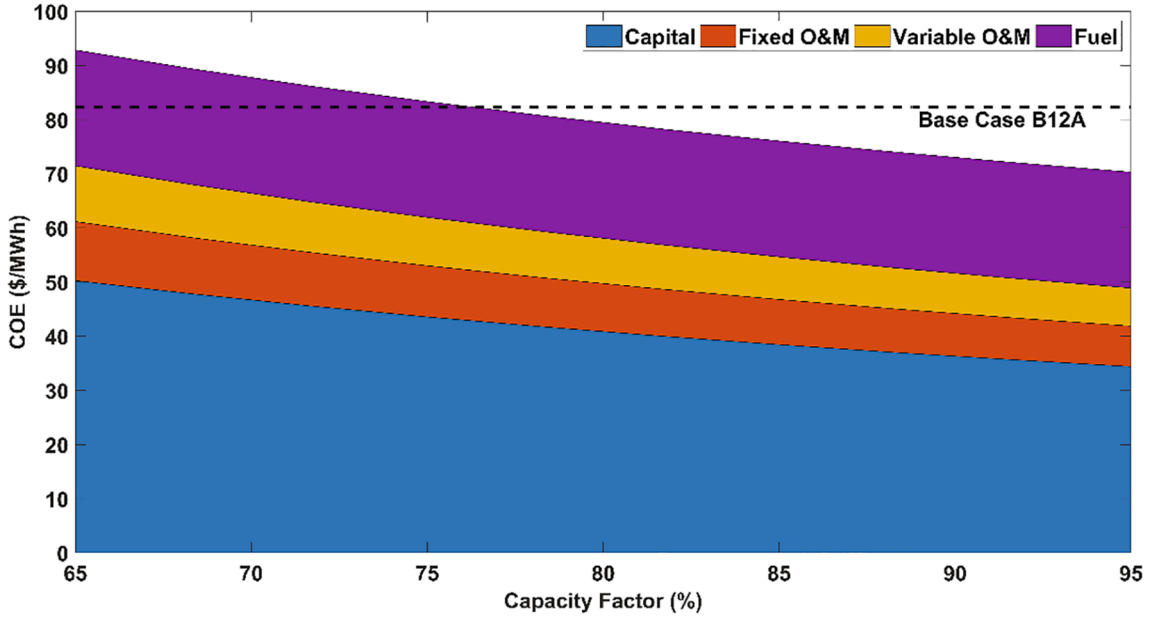

Fig. 19. Effect of plant capacity factor on COE for Case 1b.

efficiency of about 83–85% is realistically achievable for a 50 MW plant using a radial compressor. Using mean line models, Yann Le Moullec [3] indicated that using a multi-stage axial compressor can achieve 90% isentropic efficiency. Bidkar et al. [55] estimated a multi-stage turbine efficiency of about 90.6–91.6% for a 450 MW plant. A sensitivity study covering this range, of 81–91% for compressor and 80–94% for the turbine, has been evaluated. The results show that the sCO_2 cycle efficiency is more sensitive to turbine efficiency than compressor efficiency changes, as shown in Fig. 18(c), (d): this also influences the COE. The effect of compressor and turbine efficiency change on the plant efficiency and COE may also be influenced by the compressor inlet pressure and temperature, which are maintained at the same design value used in the sensitivity study.

Increasing penetration of the high volatile variable renewable energy generation units to the grid demands more flexible power generation plants suitable for cyclic operation. This reduces the plant capacity factor notably as the conventional power generation units are no longer expected to be operated in baseload [56]. Therefore, a sensitivity study is also performed for different capacity factors and the variation of COE for Case 1b is shown in Fig. 19. It should be noted that the base case B12A steam Rankine cycle assumes a capacity factor of 85%.

7. Conclusions

This work investigated the performance of four novel cycle configurations that combines the features of the partial cooling cycle, recompression cycle and cascade cycle. The thermal-economic performance of these four novel cycles is evaluated for two different turbine inlet temperatures i.e. 620 °C and 760 °C and their performance are compared with equivalent an steam Rankine cycle. The cycle configurations are modelled using in-house developed code in MATLAB® and the cycle process parameters (13–16 variables) are optimised using a genetic algorithm. sCO_2 cycles can achieve higher efficiency, in the range of 3–4% pts, which leads to a reduction of about 4–6% in the cost of electricity (COE) compared to a steam Rankine cycle (NETL base case- B12A). Increasing the turbine inlet temperature from 620 °C to 760 °C increases the efficiency further by 3–4%pts. Despite achieving higher efficiencies, the reduction in COE is smaller (1–4%) when compared with advanced ultra-supercritical steam Rankine cycle for a turbine inlet temperature of 760 °C owing to the increased capital cost from high-grade materials for the cost functions considered, making them less attractive. Increasing the number of recuperators and economisers from two to three in both recompression and partial cooling based cycles doesn't offset the COE, therefore, a simple two recuperators and economiser based configurations are recommended. Cycles derived from partial cooling cycles achieved higher efficiency and reduction in COE similar to the cycles derived from recompression cycle, therefore, partial cooling cycles can be considered owing to their higher operational freedom due to the ability in controlling the main compressor inlet pressure independent from the turbine exhaust pressure.

Since the uncertainty of sCO_2 cycle cost functions is higher owing to the lower technology readiness level, a Monte-Carlo analysis is performed to realise the associated financial risk. The Mote-Carlo analysis shows that the COE reduction range compared to steam Rankine cycle can be as high as 8%, however, this falls within the range of the cost function uncertainty i.e., the COE reduction diminishes to 0–3% at a 95-percentile cumulative probability. A sensitivity analysis shows that the turbine efficiency influences the efficiency and COE more than a compressor. For instance, the plant efficiency changes by 0.66% pts per 1% pts changes in turbine isentropic efficiency whilst it changes by 0.18% pts per 1% pts change in compressor efficiency. The boiler pressure drop affects the efficiency by 0.2% pts for 1% pts change in main heater pressure drop.

Declaration of Competing Interest

The authors declare that they have no known competing financial interests or personal relationships that could have appeared to influence the work reported in this paper.

Acknowledgements

This work was supported by the Biomass and Fossil Fuel Research Alliance (BF2RA) under grant 26-sCO_2 for efficient power generation and the Engineering and Physical Sciences Research Council, United Kingdom (EPSRC Grant No: EP/N029429/1). Data underlying this paper can be accessed at https://doi.org/10.17862/cranfield.rd.14680344.

References

[1] National Energy Technology Laboratory. Energy Storage for Fossil Fuel Energy Systems 2020. https://netl.doe.gov/coal/crosscutting/energy-storage (accessed 16 June 2020).
[2] HORIZON 2020. Supercritical CO2 Cycle for Flexible and Sustainable Support to the Electricity System 2020. https://ec.europa.eu/inea/en/horizon-2020/projects/h2020-energy/carbon-capture-storage-power-plants/sco2-flex (accessed 16 June 2020).
[3] Le Moullec Y. Conceptual study of a high efficiency coal-fired power plant with CO_2 capture using a supercritical CO_2 Brayton cycle. Energy 2013;49:32–46. https://doi.org/10.1016/j.energy.2012.10.022.
[4] Turchi CS, Ma Z, Neises T, Michael W. Thermodynamic study of advanced supercritical carbon dioxide power cycles for high performance concentrating solar power systems. Proc ASME 6th Int Conf Energy Sustain 2012;2012:375–83. https://doi.org/10.1115/ES2012-91179.
[5] Dostal V, Driscoll MJ, Hejzlar P. A Supercritical Carbon Dioxide Cycle for Next Generation Nuclear Reactors. 2004. MIT-ANP-TR-100.
[6] Thanganadar D, Asfand F, Patchigolla K. Thermal performance and economic analysis of supercritical Carbon Dioxide cycles in combined cycle power plant. Appl Energy 2019;255:113836. https://doi.org/10.1016/j.apenergy.2019.113836.
[7] Marchionni M, Bianchi G, Tassou SA. Review of supercritical carbon dioxide (sCO_2) technologies for high-grade waste heat to power conversion. SN Appl Sci 2020;2:1–13. https://doi.org/10.1007/s42452-020-2116-6.
[8] Li H, Yang Y, Cheng Z, Sang Y, Dai Y. Study on off-design performance of transcritical CO_2 power cycle for the utilization of geothermal energy. Geothermics 2018;71:369–79. https://doi.org/10.1016/j.geothermics.2017.09.002.
[9] Zhu Q. Power generation from coal using supercritical CO2 cycle Power generation from coal using supercritical CO2 cycle 2017.
[10] Crespi F, Gavagnin G, Sánchez D, Martínez GS. Supercritical carbon dioxide cycles for power generation: A review. Appl Energy 2017;195:152–83. https://doi.org/10.1016/j.apenergy.2017.02.048.
[11] Angelino G. Real Gas Effects in Carbon Dioxide Cycles. ASME- Pap 69-Gt-102 1969:1–12. 10.1115/69-GT-102.
[12] Kehlhofer R, Bahmann R, Nielsen H, Warner J. Combined-cycle gas & steam turbine power plants. second edi. PennWell 1999.
[13] Crespi F, Sánchez D, Sánchez T, Martínez GS. Capital cost assessment of concentrated solar power plants based on supercritical carbon dioxide power cycles. J Eng Gas Turbines Power 2019;141:1–9. https://doi.org/10.1115/1.4042304.
[14] Miller JD, Buckmaster DJ, Hart K, Held TJ, Thimsen D, Maxson A, et al. Turbomach. Tech Conf Expo 2017;2017:1–12. https://doi.org/10.1115/GT2017-64933.
[15] Brun K, Friedman P, Dennis R. Fundamentals and applications of supercritical carbon dioxide (sCO2) based power cycles. 2017.
[16] Held TJ. Supercritical CO_2 cycles for gas turbine combined cycle power plants. Power Gen Int 2015.
[17] Sun E, Hu H, Li H, Liu C, Xu J. How to Construct a Combined S-CO_2 Cycle for Coal Fired Power Plant? Entropy 2018;21:19. https://doi.org/10.3390/e21010019.
[18] Mohammadi K, Ellingwood K, Powell K. A novel triple power cycle featuring a gas turbine cycle with supercritical carbon dioxide and organic Rankine cycles: Thermoeconomic analysis and optimization. Energy Convers Manag 2020;220:113123. https://doi.org/10.1016/j.enconman.2020.113123.
[19] Thanganadar D, Fornarelli F, Camporeale S, Asfand F, Patchigolla K. Off-design and annual performance analysis of supercritical carbon dioxide cycle with thermal storage for CSP application. Appl Energy 2021;282:116200. https://doi.org/10.1016/j.apenergy.2020.116200.
[20] Thanganadar D, Fornarelli F, Camporeale S, Asfand F, Patchigolla K. Analysis of design, off-design and annual performance of supercritical CO2 cycles for CSP applications. Proc. ASME Turbo Expo, vol. 11, 2020. 10.1115/GT2020-14790.
[21] Zhao Q. Conception and optimization of supercritical CO_2 Brayton cycles for coal-fired power plant application. PhD Thesis. France: Université de Lorraine, Lorraine; 2018.
[22] Zhao Q, Mecheri M, Neveux T, Privat R, Jaubert J-N. Design of SC-CO2 Brayton cycles using MINLP optimization within a commercial simulator. 6th Int. Supercrit. CO2 Power Cycles Symp., Pittsburgh, Pennsylvania: 2018, p. 1–13.

[23] Mecheri M, Le Moullec Y. Supercritical CO_2 Brayton cycles for coal-fired power plants. Energy 2016;103:758–71. https://doi.org/10.1016/j.energy.2016.02.111.
[24] Bai Z, Zhang G, Li Y, Xu G, Yang Y. A supercritical CO_2 Brayton cycle with a bleeding anabranch used in coal-fired power plants. Energy 2018;142:731–8. https://doi.org/10.1016/j.energy.2017.09.121.
[25] Park SH, Kim JY, Yoon MK, Rhim DR, Yeom CS. Thermodynamic and economic investigation of coal-fired power plant combined with various supercritical CO_2 Brayton power cycle. Appl Therm Eng 2018;130:611–23. https://doi.org/10.1016/j.applthermaleng.2017.10.145.
[26] Michalski S, Hanak DP, Manovic V. Advanced power cycles for coal-fired power plants based on calcium looping combustion: A techno-economic feasibility assessment. Appl Energy 2020;269:114954. https://doi.org/10.1016/j.apenergy.2020.114954.
[27] Wei X, Manovic V, Hanak DP. Techno-economic assessment of coal- or biomass-fired oxy-combustion power plants with supercritical carbon dioxide cycle. Energy Convers Manag 2020;221:113143. https://doi.org/10.1016/j.enconman.2020.113143.
[28] Huang M, Sonwane C. Thermodynamics of conventional and non conventional sCO2 recompression Brayton cycles with direct and indirect heating. 4th Int Symp - Supercrit CO2 Power Cycles 2014:1–9. 10.1017/CBO9781107415324.004.
[29] Alfani D, Astolfi M, Binotti M, Campanari S, Casella F, Silva P. Multi objective optimization of flexible supercritical CO_2 coal-fired power plants. Proc ASME Turbo Expo 2019;3:1–11. https://doi.org/10.1115/GT2019-91789.
[30] White C, Shelton W, Dennis R. An assessment of supercritical CO_2 power cycles integrated with generic heat sources. J Chem Inf Model 2013;53:1689–99. https://doi.org/10.1017/CBO9781107415324.004.
[31] White C, Gray D, Plunkett J, Shelton W, Weiland N, Shultz T. Techno-economic evaluation of utility-scale power plants based on the indirect sCO2 Brayton cycle. 2017. 10.2172/1490272.
[32] White CW, Weiland NT, Shelton WW, Shultz TR. sCO_2 cycle as an efficiency improvement opportunity for air-fired coal combustion. 6th Int Symp - Supercrit CO2 Power Cycles 2018:1–30.
[33] Weitzel PS. Component test facility (comtest) phase 1 engineering for 760C (1400F) advanced ultra- supercritical (A-USC) steam generator development. Am Soc Mech Eng Power Div POWER 2015. https://doi.org/10.1115/POWER201549411.
[34] Nathan Weiland WS, White C. Design of a Commercial Scale Oxy-Coal Supercritical CO2 Power Cycle 2015;2015/1733.
[35] Turchi CS, Ma Z, Neises TW, Wagner MJ. Thermodynamic Study of Advanced Supercritical Carbon Dioxide Power Cycles for Concentrating Solar Power Systems. J Sol Energy Eng 2013;135:041007. https://doi.org/10.1115/1.4024030.
[36] The Babcock & Wilcox Company. Steam Its generation and use. vol. 53. 2019. 10.1017/CBO9781107415324.004.
[37] Weiland NT, Dennis RA, Ames R, Lawson S, Strakey P. Fundamentals and applications of supercritical carbon dioxide (sCO_2) based power cycles-Fossil energy. Elsevier Ltd 2017. https://doi.org/10.1016/B978-0-08-100804-1.00012-8.
[38] Purgert R, Phillips J, Tanzosh H, Shingledecker J, James. Materials for Advanced Ultra-supercritical (A-USC) Steam Turbines - A-USC Component Demonstration Pre-FEED Final Technical Report. DE-FE0026294 2016. 10.2172/1332274.
[39] Lemmon EW, Huber ML, McLinden MO. NIST Standard Reference Database 23. Natl Inst Stand Technol 2013:9.1.
[40] Fout T, Zoelle A, Keairns D, Turner M, Woods M, Kuehn N, et al. Cost and Performance Baseline for Fossil Energy Plants Volume 1a: Bituminous Coal (PC) and Natural Gas to Electricity Revision 3. Natl Energy Technol Lab 2015;1a:240. DOE/NETL-2010/1397.
[41] Nellis G, Klein S. Heat Transfer 2009. https://doi.org/10.1017/CBO9780511841606.
[42] Schmitt J, Wilkes J, Bennett J, Wygant K, Pelton R. Lowering the levelized cost of electricity of a concentrating solar power tower with a supercritical carbon dioxide power cycle. ASME Turbo Expo, Charlotte, NC, USA: 2017, p. 1–10. 10.1115/GT2017-64958.
[43] White CW, Shelton WW, Weiland NT, Shultz TR. sCO2 Cycle as an Efficiency Improvement Opportunity for Air-fired Coal Combustion. 2018. 10.2172/1511695.
[44] Laboratory NET. Quality Guidelines for Energy System Studies: Capital Cost Scaling Methodology. 2013. https://doi.org/10.2172/1513277.
[45] National Energy Technology Laboratory. Quality Guideline for Energy System Studies: Cost Estimation Methodology for NETL Assessments of Power Plant Performance. 2019.
[46] Carlson MD, Middleton BM, Ho CK. Techno-Economic Comparison of Solar-Driven sCO2 Brayton Cycles Using Component Cost Models Baselined With Vendor Data. Proc ASME 2017 Power Energy Conf 2017:1–7. 10.1115/ES2017-3590.
[47] Weiland NT, Lance BW, Pidaparti SR. SCO2 power cycle component cost correlations from DOE data spanning multiple scales and applications. Proc. ASME Turbo Expo, vol. 9, 2019, p. 1–17. 10.1115/GT2019-90493.
[48] Couper JR, Penney WR, Fair JR, Walas SM. Chemical process equipment: Selection and design. Third Edit 2012. https://doi.org/10.1016/B978-0-12-396959-0.00025-2.
[49] Moisseytsev A, Sienicki JJ. Investigation of alternative layouts for the supercritical carbon dioxide Brayton cycle for a sodium-cooled fast reactor presentsation. Nucl Eng Des 2009;239:1362–71. https://doi.org/10.1016/j.nucengdes.2009.03.017.
[50] Spelling J. drawSankey (https://www.mathworks.com/matlabcentral/fileexchange/26573-drawsankey). MATLAB Cent File Exch 2021.
[51] Fleming DD, Conboy TM, Pasch JJ, Rochau GA, Fuller RL, Holschuh TV, et al. Scaling Considerations for a Multi- Megawatt Class Supercritical CO_2 Brayton Cycle and Commercialization. Sandia Rep 2013.
[52] A.Bidkar R. Conceptual Designs of 50MW and 450 MW supercritical CO2 Turbomachinery Trains for Power Generation from Coal.Part2: Compressors. 5th Int. Symp. - Supercrit. CO2 Power Cycles, San Antonio, Texas, USA: 2016, p. 1–18.
[53] Weiland N, Thimsen D. A Practical Look at Assumptions and Constraints for Steady State Modeling of sCO_2 Brayton Power Cycles. In: 5th Int SCO2 Symp; 2016. p. 1–14.
[54] Noall JS, Pasch JJ. Achievable Efficiency and Stability of Supercritical CO_2 Compression Systems Main Compressor Design Discussion. In: 4th Int Symp - Supercrit CO2 Power Cycles Sept; 2014, 2014,. p. 1–10.
[55] Bidkar RA, Mann A, Singh R, Sevincer E, Cich S, Day M, et al. Conceptual Designs of 50MWe and 450MWe Supercritical CO2 Turbomachinery Trains for Power Generation from Coal. Part 1: Cycle and Turbine. 5th Int Symp - Supercrit CO2 Power Cycles 2016:17.
[56] NREL. Renewable Electricity Futures Study: Executive Summary. vol. 1. 2012. NREL/TP-6A20-52409-1.

https://dspace.org/

Techno-economic analysis of supercritical carbon dioxide cycle integrated with coal-fired power plant

Thanganadar, Dhinesh; Asfand, Faisal; Patchigolla, Kumar; Turner, Peter J.

2021-05-30
Elsevier
https://doi.org/10.1016/j.enconman.2021.114294
Thanganadar D, Asfand F, Patchigolla K, Turner P. (2021) Techno-economic analysis of supercritical carbon dioxide cycle integrated with coal-fired power plant. Energy Conversion and Management, Volume 242, August 2021, Article number 114294

Downloaded from a DSpace repository. https://dspace.org/